



OPEN ACCESS

EDITED BY

Marina Caputo,
Università degli Studi del Piemonte
Orientale, Italy

REVIEWED BY

Rui Liu,
Hunan Provincial People's Hospital, China
Ludovico Docimo,
University of Campania Luigi Vanvitelli, Italy

*CORRESPONDENCE

Kai Wang

✉ wangkaimath@sina.com

Li Ma

✉ malixj322122@gmail.com

[†]These authors have contributed equally to this work

RECEIVED 04 March 2024

ACCEPTED 07 October 2024

PUBLISHED 28 October 2024

CITATION

Huang Y, Lou P, Li H, Li Y, Ma L and Wang K (2024) Risk nomogram for papillary thyroid microcarcinoma with central lymph node metastasis and postoperative thyroid function follow-up. *Front. Endocrinol.* 15:1395900. doi: 10.3389/fendo.2024.1395900

COPYRIGHT

© 2024 Huang, Lou, Li, Li, Ma and Wang. This is an open-access article distributed under the terms of the [Creative Commons Attribution License \(CC BY\)](https://creativecommons.org/licenses/by/4.0/). The use, distribution or reproduction in other forums is permitted, provided the original author(s) and the copyright owner(s) are credited and that the original publication in this journal is cited, in accordance with accepted academic practice. No use, distribution or reproduction is permitted which does not comply with these terms.

Risk nomogram for papillary thyroid microcarcinoma with central lymph node metastasis and postoperative thyroid function follow-up

Yuting Huang^{1†}, Pengwei Lou^{2†}, Hui Li³, Yinhui Li³, Li Ma^{3*} and Kai Wang^{4*}

¹Department of Medical Administration, Traditional Chinese Medicine Hospital Affiliated to Xinjiang Medical University, Urumqi, China, ²Department of Big Data, College of Information Engineering, Xinjiang Institute of Engineering, Urumqi, China, ³Department of Endocrine, Traditional Chinese Medicine Hospital Affiliated to Xinjiang Medical University, Urumqi, China, ⁴College of Public Health, Xinjiang Medical University, Urumqi, China

Background: The treatment for papillary thyroid microcarcinoma (PTMC) is controversial. Central lymph node metastasis (CLNM) is one of the main predictors of recurrence and survival, accurate preoperative identification of CLNM is essential for surgical protocol establishment for PTMC. The objective of this study was to establish a nomogram to predict the possibility of CLNM in PTMC patients.

Methods: A total of 3023 PTMC patients were randomly divided into two groups by a ratio of 7 to 3, the training group (n = 2116) and validation group (n = 907). The LASSO regression model and multivariate logistic regression analysis were performed to examine risk factors associated with CLNM. A nomogram for predicting CLNM was established and internally validated. Meanwhile, we follow-up the serum thyroid function FT3, FT4, TSH, Tg, TGAb and TPOAb in 789 PTMC patients for 4 years after surgery and compared the differences between the CLNM (+) and CLNM (-) groups, respectively.

Results: The LASSO regression model and multivariate logistic regression analysis showed that younger age, lower BMI, being male, location in the lower pole, calcification, $1 \geq \text{diameter} \geq 0.5$ cm, multifocality lesions, extra thyroidal extension (ETE), enlargement of central lymph node (ECLN), lateral lymph node metastasis (LLNM) and higher carcinoembryonic antigen were the ultimate risk factors for determining CLNM. A nomogram for predicting CLNM was constructed based on the influencing factors and internally validated. By establishing the prediction model, the AUC of CLNM in the training and validation groups were 0.73 (95% CI, 0.70-0.76) and 0.75 (95% CI, 0.71-0.79) respectively. Results of the DCA showed that the model is clinically useful when deciding on intervention in the most range of the threshold probability. A 4-year follow-up of thyroid function showed that FT3 and FT4 remained at stable levels after 3 months postoperative and were higher in the CLNM (+) group than in the CLNM (-) group. Hypothyroidism appeared predominantly within 3 months after surgery. The overall incidence of the CLNM (+) group and CLNM (-) groups were 16.46% and 12.04%, respectively.

Conclusion: The nomogram model constructed in this study has a good predictive effect on CLNM in PTMC patients and provides a reasonable reference for clinical treatment.

KEYWORDS

papillary thyroid microcarcinoma, central lymph node metastasis, risk factors, nomogram, thyroid function

Introduction

Papillary thyroid microcarcinoma (PTMC) is defined as malignant thyroid tumors of ≤ 1 cm in diameter, which accounts for approximately 30–60% of the papillary thyroid carcinoma (PTC) (1–3). In recent years, the incidence of thyroid microcarcinoma has increased rapidly, mainly attributed to the application of routine high-resolution ultrasonography (USG) and other imaging techniques (4). In the 5th edition of the WHO classification criteria for thyroid tumors, the subtype classification based on tumor size has been eliminated, mainly due to the fact that factors such as pathological subtypes, aggressiveness, and lymph node metastasis of thyroid cancer have a greater impact on the prognosis, and physicians develop individualized treatment plans accordingly (5).

Most PTMCs are known to be inert and have a favorable prognosis, with a long-term survival rate of exceeding 99% (6). However, some PTMCs still have high-risk features at the time of diagnosis, for example, cervical lymph node metastasis and extrathyroidal extension (ETE) are closely associated with an increased risk of distant metastasis, high local recurrence, and death (3, 7). Central lymph node metastasis (CLNM) was found in 40–60% of PTMC patients in most series by using standard pathology technique (8, 9). The 2015 American Thyroid Association (ATA) guidelines for differentiated thyroid cancer stated that central lymph node dissection (CLND) should be considered when the preoperative ultrasound shows a significant metastatic lymph node (cN1) or if they are palpable at the time of examination. Routine prophylactic CLND is not recommended for non-invasive, T1 or T2 and clinically node-negative (cN0) PTC (10). The need for routine prophylactic CLND in patients without clinical evidence of CLNM, especially for those with unilateral lesions, remains controversial (11).

The Chinese and Japanese PTC guidelines recommend that prophylactic CLND should adequately protect the parathyroid gland and the recurrent laryngeal nerve (RLN) (12, 13). Considering the prediction of CLNM is critical in potentially deciding on the surgical approach. Therefore, it is crucial to accurately assess the status of the cervical lymph nodes. Although preoperative high-resolution ultrasound (HUS) plays an important role in CLNM evaluation, it has quite low sensitivity (14). Therefore, it is of great significance to develop a new method for

accurately evaluating the status of the cervical lymph nodes, in order to provide guidance for a personalized surgical approach. Many studies have reported on the preoperative clinicopathologic risk factors of CLNM for PTMC, but the results are inconsistent (15–17).

Some studies have only predicted risk factors for CLNM in patients with PTMC, but long-term follow-up studies of thyroid function after surgery are scarce (18, 19). Currently, there are no comprehensive and systematic reports on the prediction of preoperative CLNM risk, postoperative trends in thyroid function indicators and complication rates in patients with PTMC, especially comparing the differences between CLNM (+) (represents the occurrence of CLNM) and CLNM (–) (indicates that no CLNM occurred) groups have hardly reported, which is a limitation for PTMC patients to understand their postoperative progression.

The aim of our study was to establish a practical nomogram for preoperative prediction of the likelihood of CLNM based on clinical, hematological, USG and pathological features in order to determine the surgical extent and therapeutic strategy for patients with PTMC. We also analyzed the trends of postoperative thyroid function indicators, the incidence of postoperative complications of subclinical hypothyroidism and hypothyroidism, and compared the differences between the CLNM (+) and CLNM (–) groups, which provided a reference for clinicians to develop postoperative treatment plans.

Materials and methods

Study design and participants

Clinical case data of patients who underwent thyroid surgery and were diagnosed with PTMC postoperatively from January 2015 to December 2022 in Traditional Chinese Medicine Hospital of Xinjiang Medical University were retrospectively selected. The variables included patient age, sex, BMI, maximum tumor size, history at diagnosis, thyroid function, USG parameters, pathological results and other indicators. The exclusion criteria were as follows: (1) patients who underwent secondary or further thyroid surgery; (2) patients who did not undergo radical surgery or CLND; (3) previously diagnosed other concomitant malignancies, such as breast cancer, lung cancer, colon cancer, and other cancers;

(4) patients who also had other types of thyroid carcinoma, such as medullary, follicular and anaplastic thyroid carcinomas; (5) clinically and/or pathologically detected distant metastasis, such as secondary malignant tumor of bone, liver, and other body parts; (6) patients lost to follow-up or with incomplete clinical information.

Information collection

The possible risk factors of PTMC with CLNM analyzed in this study can be divided into 4 categories including 40 variables.

The general clinical conditions include: gender, age, ethnicity, marital status, body mass index (BMI), diabetes, heart disease, smoking, drinking, family history of cancer, family history of thyroid disease. All of these factors can be obtained from hospitalized records.

Biochemical variables recorded include thyroid function [free triiodothyronine (FT3), free thyroxine (FT4), thyroid stimulating hormone (TSH), thyroglobulin (Tg)], thyroid antibody [thyrotropin receptor antibody (TRAb), Anti-thyroglobulin antibodies (TgAb), thyroid peroxidase antibodies (TPOAb)], blood lipid [triglyceride (TG), cholesterol (CHOL)], tumor markers [alpha fetoprotein (AFP), carcinoembryonic antigen (CEA), calcitonin (Ct)]. The results of these biochemical indicators are exported from the hospital information system.

A GE-E11 ultrasound system (GE Medical System, USA) with a linear array probe was used to acquire ultrasound images in the frequency range of 9-11MHz. All patients were in the supine position with the lower shoulder pillow neck extended to better expose the inferior thyroid rim. Both thyroid lobes and isthmus of the thyroid were scanned in the transverse and longitudinal planes. Longitudinal and transverse images of the thyroid were obtained according to American College of Radiology accreditation standards. The thyroid nodule ultrasound chart was prejudged by two experienced sonographers.

The following USG parameters of the nodules were recorded as follows: (1) margin, (2) shape, (3) echogenicity, (4) calcification, (5) diffuse, (6) color doppler flow imaging (CDFI), (7) tumor position: location_Upper/Middle/Lower, location_Left/Right/Isthmus, (8) ECLN.

The clinicopathological test results included: (1) diameter, (2) hashimoto thyroiditis, (3) nodular goiter, (4) ETE, (5) multifocality, (6) bilateral, (7) lateral lymph node metastasis (LLNM). Postoperative histopathologic evaluations were performed by pathologists experienced in thyroid pathology.

This judgement criteria of the study were as follows: (1) malignant tumors were considered to be multifocal when more than one malignant tumor foci were found in the same or different lobes of the gland; (2) if the same patient had multiple lesions, the malignant tumor with the largest diameter was selected as the research object. When the diameter was the same, the higher Thyroid Imaging Reporting and Data System (TI-RADS) level would be selected. The maximum tumor diameter was categorized in two groups: the small group (< 0.5 cm) and the large group (0.5-1.0 cm); (3) ETE was confirmed when there was evidence of a malignant tumor invading

adipose tissue, banded muscle, larynx, trachea, esophagus, recurrent laryngeal nerve, prevertebral fascia or blood vessels; (4) lateral lymph node dissection (LLND), including levels II-V, was performed only in cases with clinically evident lateral neck lymph node metastasis. Assessed by the experienced physician, the patients without LLND were classified as non-occurrence LLNM; (5) the range of TgAb and TPOAb actual detection results is wide, being 0-4000 IU/ml and 0-600 IU/ml respectively. In this study, these were set as dichotomous variables: TgAb was divided into Normal (≤ 115 IU/ml) and Abnormal (> 115 IU/ml) groups; TPOAb was also divided into Normal (≤ 34 IU/ml) and Abnormal (> 34 IU/ml) groups.

Follow-up of thyroid function indicators

In order to clarify the trend of thyroid function in PTMC patients at different postoperative periods and to compare the differences between the CLNM (+) and the CLNM (-) groups, thyroid function indicators were retrospectively collected in this study. FT3, FT4, TSH, Tg, TgAb, and TPOAb in PTMC patients during the following consecutive periods: preoperatively, within 3 days, 1 month, 3 months, 6 months, 1 year, 2 years, 3 years, and 4 years postoperatively. By the end of 2022, those eligible for follow-up 4 years thyroid function indicator data were PTMC patients who underwent surgery during 2015-2018. Data were obtained from thyroid function markers at the time the patients underwent regular follow-up of patients during outpatient or hospitalization. Patients with omissions or missing data are excluded, and those with high compliance, completeness, and continuity of thyroid function indicators were retained for analysis. In accordance with guidelines for the diagnosis and management of subclinical thyroid disorders and the standard practices in hospital laboratories, the normal ranges of thyroid function indicators were determined as follows: $3.1 \leq FT3 \leq 6.8$ pmol/L, $12 \leq FT4 \leq 22$ pmol/L, $0.27 \leq TSH \leq 4.2$ uIU/ml, $3.5 \leq Tg \leq 77$ ng/ml, $0 \leq TgAb \leq 115$ IU/ml, $0 \leq TPOAb \leq 34$ IU/ml. Subclinical hypothyroidism is defined as an elevation in serum TSH level above the upper limit of the reference range and a normal FT4 level. Overt hypothyroidism is defined as an increase in serum TSH level and a decrease in FT4 level.

Data screening

Between January 2015 and December 2022, there were 7005 thyroid surgery in-patients based on the medical record data of Traditional Chinese Medicine Hospital Affiliated to Xinjiang Medical University. According to strict exclusion criteria, 3023 PTMC cases were included in this study in the end, 621 had CLNM, as shown in [Figure 1](#). To better verify the predictive power of the model and to analyze the possibility of CLNM in PTMC, 3023 cases were randomly divided into two groups by a ratio of 7 to 3, 2116 were in the training group and 907 in the validation group.

A total of 789 patients with complete serum thyroid function indicators at 4-year postoperative follow-up among the patients

with PTMC, including 158 with CLNM (+) and 631 with CLNM (-), as shown in **Figure 1**. There were 1424 eligible patients for PTMC surgery from 2015-2018, with a complete follow-up rate of 55.41%.

The study was approved by the Medical Ethics Committee of Traditional Chinese Medicine Hospital Affiliated to Xinjiang Medical University (IRB No. 2022XE0171). All participants gave written informed consent for their clinical records to be used in this study.

Thyroid surgery and pathologic analysis

During surgery, the tumors were sent for frozen sections and confirmed as PTMC. After rediagnosis, these patients underwent thyroidectomy and cervical lymph node dissection, and the lymph nodes were sent for frozen sections to confirm CLNM and LLNM. After surgery, the remaining specimens were sent for paraffin sections for final confirmation of PTMC, CLNM and LLNM. Two or more experienced pathologists microscopically reviewed and cross-checked all pathology specimens. Principles of

thyroidectomy: total thyroidectomy was performed in patients with extraglandular invasion, bilateral or multiple lesions, and bilateral cervical lymph node metastases, and ipsilateral and isthmus resection were performed in patients with unilateral intrathyroidal tumors. Principles of cervical lymph node dissection: central lymph nodes (level VI) were routinely dissection, and lateral compartment lymph nodes (levels II-V) with evidence of lymph node metastasis should be dissection. Upper mediastinal lymph nodes (level VII) should be also cleared if there are enlarged lymph nodes based on neck imaging. The recurrent laryngeal nerves should be directly visualized throughout the node clearance process to avoid injury. The parathyroid gland and their blood supply should be retained.

A total of 3023 patients with PTMC who underwent surgical treatment were included in this study, of which 1360 patients underwent total thyroidectomy, 1341 patients underwent unilateral lobectomy + isthmus resection, 314 patients underwent unilateral lobectomy + isthmus + partial resection of contralateral lobectomy, and 8 patients underwent bilateral partial lobectomy + isthmus resection. Lymph node dissection was performed in zone

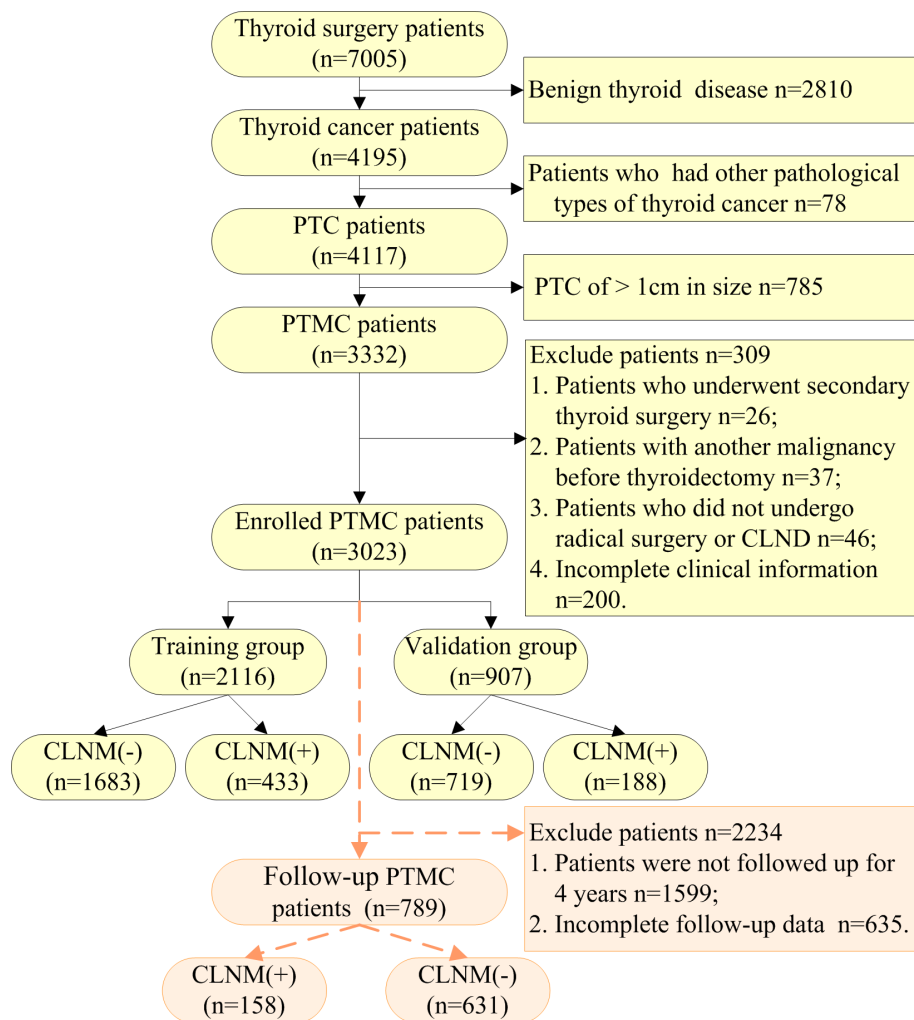


FIGURE 1
Flow diagram of the data screening.

VI only in 2798 patients (ipsilateral 1164 patients and bilateral 1154 patients) and in zones II, III, IV and VI in 224 patients (ipsilateral 5 patients and bilateral 219 patients).

Statistical analysis

The open source R software, Version 4.3.3 (<https://www.r-project.org>) and the Statistical Package for the Social Sciences (SPSS) for Windows, Version 21.0 (SPSS Inc., Chicago, IL, United States) were used for data analysis and modeling in this study. When contrasting the baseline information and clinical features between the modeling group and the control group, the chi-square test or Fisher's exact test were used for categorical variables, expressed by actual cases and percentages (%); the student's t-test or Wilcoxon rank sum test was used for continuous variables, shown by mean \pm standard deviation (SD). After assessing risk factors by the least absolute shrinkage and selection operator (LASSO) regression model, the non-zero variate was considered significant. A multivariate logistic regression model for prediction was then established, and the coefficient, odds ratio (OR) with 95% confidence interval (CI) and *p*-values of variables were established at the same time; the statistical significance variables (*p*-values < 0.05) were the influence factors. All statistical tests were two sided, and *p*-values < 0.05 were considered statistically significant.

A nomogram, based on influencing factors determined by the multivariate logistic regression model, was established by rms/PROC pack in R software, which was used to evaluate the risk of CLNM preoperatively and gave every variable to a score between 0 and 100. The goodness of fit test of the model between modeling and validation groups was assessed by receiver operating characteristic (ROC) curve and calibration curve. The ROC curve was plotted to quantify and contrast the risk of PTMC with CLNM between forecasting and observing cases. The reasonable range of area under ROC curve (AUC) is 0.5 to 1, the closer the value is to 1, the stronger the model prediction ability. The calibration curve, as a very important criteria, was used to assess how well the model fits the real data. Our conclusion from the contained 1000 bootstrap samples: the smaller the mean absolute error, the higher the accuracy in forecasting was. Vice versa, the lower accuracy showed the model may over- or underestimate the risk of illness. A Hosmer-Lemeshow goodness-of-fit test was also performed to assess predictive ability; the larger the *p*-value, the better the predictive ability. The DCA was drawn to make the clinical decision benefit in predicting the risk of PTMC with CLNM.

Results

Baseline characteristics

In our study, a total of 3023 PTMC patients were recruited according to the inclusion and exclusion criteria; the average age was 47.33 ± 10.39 years, there were 2381 (78.76%) females and 642 (21.24%) males (ratio 3.71:1). CLNM and non-CLNM were observed in 621 (20.54%) and 2402 (79.46%) cases respectively.

A total of 2116 patients with PTMC were included in the training group consisting of 1665 (78.69%) females and 451 (21.31%) males (ratio 3.69:1), and the average age was 47.27 ± 10.44 years. CLNM and non-CLNM were observed in 433 (20.46%) and 1683 (79.54%) cases respectively. Meanwhile, 907 PTMC patients were assigned to the validation group, there were 716 (78.94%) females and 191 (21.06%) males (ratio 3.75:1), and the average age was 47.46 ± 10.27 years. CLNM and non-CLNM were observed in 188 (20.73%) and 719 (79.27%) cases respectively.

We collected 43 indexes to identify the risk factors for CLNM in PTMC. There were no statistically significant differences ($P > 0.05$) in general clinical data, biochemical indicators, ultrasonic characteristics and clinicopathological results between the training and the validation group, except for the Ct, as shown in [Table 1](#).

Characteristics selection

For the study, the LASSO regression was used for feature selection in the training group. With the change of the penalty coefficient λ , the variables included in the model were gradually reduced. The λ in the LASSO model was selected via tenfold-validation based on minimum criteria ($\lambda_{\min} = 0.0099$). At the same time, 18 non-zero coefficient characteristics ([Figures 2A, B](#)) were selected to build the multivariate logistic regression analysis, including age, gender, BMI, marital status, hashimoto thyroiditis, location_UML, calcification, diameter, multifocality, ETE, ECLN, LLNM, TG, FT3, TSH, Tg, TPOAb, CEA.

The multivariate logistic regression analysis concluded that younger age (OR = 1.02, 95% CI, 1.01-1.03, $P < 0.001$), Lower BMI (OR = 1.03, 95% CI, 1.00-1.07, $P = 0.049$), being male (OR = 1.56, 95% CI, 1.16-2.09, $P = 0.003$), location in lower pole (OR = 1.43, 95% CI, 1.04-1.96, $P = 0.028$), calcification (OR = 1.34, 95% CI, 1.06-1.69, $P = 0.015$), $1 \geq \text{diameter} \geq 0.5$ cm (OR = 1.78, 95% CI, 1.38-2.31, $P < 0.001$), multifocality lesions (OR = 1.64, 95% CI, 1.28-2.10, $P < 0.001$), ETE (OR = 1.47, 95% CI, 1.02-2.09, $P = 0.035$), ECLN (OR = 1.65, 95% CI, 1.18-2.29, $P = 0.003$), LLNM (OR = 5.47, 95% CI, 3.55-8.51, $P < 0.001$) and CEA (OR = 1.18, 95% CI, 1.05-1.32, $P = 0.003$) were the independent risk factors of PTMC patients with CLNM. It should be emphasized that age (-) and BMI (-) were correlated with CLNM negatively, the higher the value, the lower the risk of CLNM. We calculated the risk value of Age (+) and BMI (+) by conversion of the dependent variables. The detailed results are shown in [Figure 3](#). Meanwhile, we list the distribution characteristics of the 11 risk factors in CLNM (+) group and CLNM (-) group respectively in [Table 2](#). The differences were statistically significant ($P < 0.05$).

Nomogram of CLNM in PTMC patients

Based on LASSO and multivariate logistic regression analysis, we produced a nomogram model consisting of 11 factors, which were used to estimate the risk of CLNM in PTMC patients. According to the scored ruler as shown in [Figure 4](#), each variety has a corresponding point value on each variable axis: all the points were added up to obtain the overall points. The sum of these

TABLE 1 Baseline clinical characteristics in patients with PTMC.

Characteristics	Total n = 3023	Training group n = 2116	Validation group n = 907	χ^2 or t-test	P value
Group				0.027	0.869
CLNM (+)	621 (20.54)	433 (20.46)	188 (20.73)		
CLNM (-)	2402 (79.46)	1683 (79.54)	719 (79.27)		
Gender				0.025	0.875
Male	642 (21.24)	451 (21.31)	191 (21.06)		
Female	2381 (78.76)	1665 (78.69)	716 (78.94)		
Age (years)	47.33 ± 10.39	47.27 ± 10.44	47.46 ± 10.27	0.478	0.633
BMI (kg/m ²)	24.91 ± 3.54	24.91 ± 3.55	24.90 ± 3.51	-0.028	0.978
Ethnicity				0.022	0.989
Han	2334 (77.21)	1635 (77.27)	699 (77.07)		
Uygur	313 (10.35)	218 (10.30)	95 (10.47)		
Other nationalities	376 (12.44)	263 (12.43)	113 (12.46)		
Marital status				2.975	0.226
Single	118 (3.90)	91 (4.30)	27 (2.98)		
Married	2768 (91.57)	1929 (91.16)	839 (92.50)		
Divorced/Windowed	137 (4.53)	96 (4.54)	41 (4.52)		
Smoking				0.060	0.807
Yes	317 (10.49)	220 (10.39)	97 (10.69)		
No	2706 (89.51)	1896 (89.61)	810 (89.31)		
Drinking				1.373	0.241
Yes	275 (9.10)	184 (8.70)	91 (10.03)		
No	2748 (90.90)	1932 (91.30)	816 (89.97)		
Hashimoto thyroiditis				0.264	0.607
Yes	762 (25.21)	539 (25.47)	223 (24.59)		
No	2261 (74.79)	1577 (74.53)	684 (75.41)		
Nodular goiter				0.740	0.390
Yes	1222 (40.42)	866 (40.93)	356 (39.25)		
No	1801 (59.58)	1250 (59.07)	551 (60.75)		
Hypertension				0.003	0.960
Yes	655 (21.67)	459 (21.69)	196 (21.61)		
No	2368 (78.33)	1657 (78.31)	711 (78.39)		
Diabetes				0.227	0.634
Yes	285 (9.43)	203 (9.59)	82 (9.04)		
No	2738 (90.57)	1913 (90.41)	825 (90.96)		
Heart disease				3.243	0.072
Yes	193 (6.38)	124 (5.86)	69 (7.61)		
No	2830 (93.62)	1992 (94.14)	838 (92.39)		
Family history of cancer				0.140	0.708

(Continued)

TABLE 1 Continued

Characteristics	Total n = 3023	Training group n = 2116	Validation group n = 907	χ^2 or t-test	P value
Yes	468 (15.48)	331 (15.64)	137 (15.10)		
No	2555 (84.52)	1785 (84.36)	770 (84.90)		
Family history of thyroid disease				0.016	0.899
Yes	75 (2.48)	52 (2.46)	23 (2.54)		
No	2948 (97.52)	2064 (97.54)	884 (97.46)		
Diameter (cm)	0.52 ± 0.25	0.52 ± 0.25	0.51 ± 0.25	-0.784	0.433
< 0.5	1259 (41.65)	878 (41.49)	381 (42.01)	0.069	0.793
0.5-1	1764 (58.35)	1238 (58.51)	526 (57.99)		
ETE				0.347	0.556
Yes	281 (9.30)	201 (9.50)	80 (8.82)		
No	2742 (90.70)	1915 (90.50)	827 (91.18)		
LLNM				0.231	0.631
Yes	159 (5.26)	114 (5.39)	45 (4.96)		
No	2864 (94.74)	2002 (94.61)	862 (95.04)		
ECLN				3.818	0.051
Yes	357 (11.81)	234 (11.06)	123 (13.56)		
No	2666 (88.19)	1882 (88.94)	784 (86.44)		
Bilateral				0.535	0.465
Yes	513 (16.97)	366 (17.30)	147 (16.21)		
No	2510 (83.03)	1750 (82.70)	760 (83.79)		
Multifocality				0.665	0.415
Yes	763 (25.24)	543 (25.66)	220 (24.26)		
No	2260 (74.76)	1573 (74.34)	687 (75.74)		
Location_UML				0.122	0.941
Upper pole	652 (21.57)	457 (21.60)	195 (21.50)		
Middle third	1226 (40.56)	854 (40.36)	372 (41.01)		
Lower pole	1145 (37.87)	805 (38.04)	340 (37.49)		
Location_LRI				2.172	0.337
Left lobe	1385 (45.82)	952 (45.00)	433 (47.74)		
Right lobe	1525 (50.45)	1086 (51.32)	439 (48.40)		
Isthmus	113 (3.73)	78 (3.68)	35 (3.86)		
Diffuse				0.447	0.504
Yes	511 (16.90)	364 (17.20)	147 (16.21)		
No	2512 (83.10)	1752 (82.80)	760 (83.79)		
Echogenicity				0.080	0.778
Hypoechoic	3008 (99.50)	2106 (99.53)	902 (99.45)		
Isoechoic/Hyperechoic	15 (0.50)	10 (0.47)	5 (0.55)		
Margin				0.837	0.360

(Continued)

TABLE 1 Continued

Characteristics	Total n = 3023	Training group n = 2116	Validation group n = 907	χ^2 or t-test	P value
Clear	852 (28.18)	586 (27.69)	266 (29.33)		
Unclear	2171 (71.82)	1530 (72.31)	641 (70.67)		
Shape				2.763	0.096
Regular	463 (15.32)	309 (14.60)	154 (16.98)		
Irregular	2560 (84.68)	1807 (85.40)	753 (83.02)		
CDFI				0.239	0.625
Yes	1626 (53.79)	1132 (53.50)	494 (54.47)		
No	1397 (46.21)	984 (46.50)	413 (45.53)		
Calcification				0.113	0.737
Yes	1083 (35.83)	754 (35.63)	329 (36.27)		
No	1940 (64.17)	1362 (64.37)	578 (63.73)		
TG (mmol/L)	1.49 ± 1.01	1.50 ± 1.04	1.46 ± 0.94	-1.163	0.245
CHOL (mmol/L)	4.41 ± 0.92	4.41 ± 0.93	4.40 ± 0.90	-0.097	0.923
FT3 (pmol/L)	4.63 ± 1.01	4.63 ± 1.05	4.63 ± 0.92	-0.167	0.868
FT4 (pmol/L)	15.84 ± 3.08	15.82 ± 3.17	15.88 ± 2.84	0.451	0.652
TSH (uIU/ml)	2.67 ± 2.17	2.66 ± 2.14	2.69 ± 2.23	0.435	0.664
Tg (ng/ml)	21.34 ± 51.34	21.45 ± 50.81	21.06 ± 52.56	-0.192	0.847
TRAb (IU/L)	0.69 ± 1.30	0.68 ± 1.24	0.70 ± 1.42	0.309	0.757
TgAb (IU/ml)	105.83 ± 334.89	103.75 ± 323.43	110.65 ± 360.36	0.518	0.604
Normal [\leq 115]	2506 (82.90)	1748 (82.61)	758 (83.57)	0.416	0.519
Abnormal [$>$ 115]	517 (17.10)	368 (17.39)	149 (16.43)		
TPOAb (IU/ml)	44.43 ± 98.23	42.88 ± 94.91	48.01 ± 105.54	1.260	0.208
Normal [\leq 34]	2509 (83.00)	1758 (83.08)	751 (82.80)	0.035	0.851
Abnormal [$>$ 34]	514 (17.00)	358 (16.92)	156 (17.20)		
AFP (ng/ml)	3.36 ± 2.76	3.33 ± 2.23	3.42 ± 3.73	0.803	0.508
CEA (ng/ml)	1.56 ± 1.06	1.54 ± 1.01	1.58 ± 1.17	0.839	0.402
Ct (pg/ml)	1.19 ± 1.92	1.23 ± 2.15	1.10 ± 1.21	-2.112	0.035

numbers is located on the total points axis to express the incidence of the risk for CLNM. The higher the total points, the greater the possibility of CLNM risk. In this study, the risk of PTMC combined with CLNM ranged from 0% to 90%, as assessed by 11 risk factors.

Validation of nomogram for the CLNM

The ROC curve was drawn to predict the nomogram effect (Figures 5A, B). The area under the ROC curve (AUC) of the training group was 0.73 (95% CI, 0.70-0.76), the diagnostic cut-off point was 0.21 (sensitivity, 0.61, specificity, 0.74). The AUC of the validation group was 0.75 (95% CI, 0.71-0.79), the diagnostic cut-off

point was 0.24 (sensitivity, 0.56, specificity, 0.81). In addition, the AUC value of the validation group was only 0.02 higher than that of the training group, which indicates that the model has good prediction discrimination in both groups.

The calibration plots present a good agreement between the actual and predicted metastasis probability with an additional 1000 bootstraps, the mean absolute error of the training and validation groups were 0.015 and 0.012, respectively (Figures 6A, B). Meanwhile, the calibration of the prediction model was evaluated by Hosmer-Lemeshow goodness of fit test: when $P > 0.05$, the calibration ability of the model is good. The P values of the training and validation groups calibration curves were 0.95 and 0.60, respectively, which indicated that the nomogram model was well consistent between prediction and actual values.

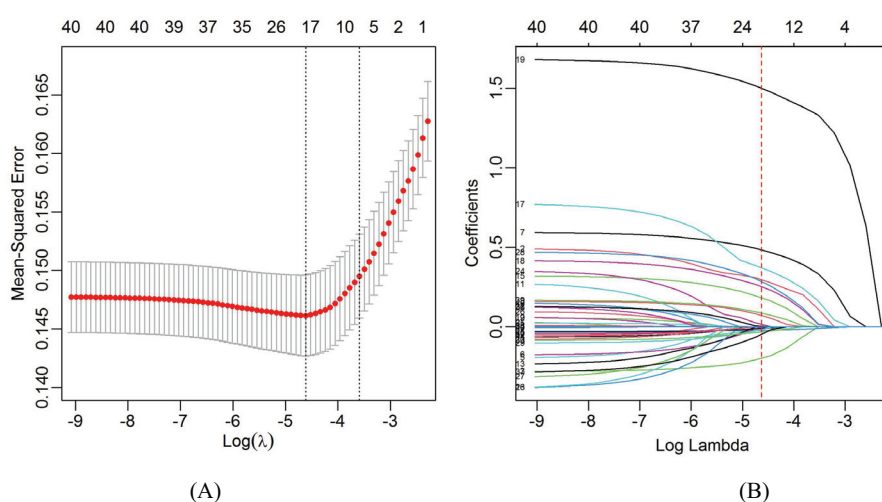


FIGURE 2

Demographic and clinical feature selection using the least absolute shrinkage and selection operator (LASSO) binary logistic regression model.

(A) Optimal parameters (λ) selection in the LASSO model used tenfold cross-validation via minimum criteria. The Mean-Squared Error was plotted as a function of $\log(\lambda)$. The dotted red curve indicates the average Mean-Squared Error values. The area under the receiver operation characteristic curve was plotted versus $\log(\lambda)$. Dotted vertical lines were plotted at the optimal values by using the minimum criteria and the 1 standard error of the minimum criteria. (B) LASSO coefficient profiles of the 20 features. A coefficient profile plot was produced against the $\log(\lambda)$ sequence. A vertical line was plotted at the value selected using tenfold cross validation, where optimal lambda resulted in 20 features with non-zero coefficients.

DCA curve of the nomogram

Results of DCA in training and validation groups were shown in Figures 7A, B. The DCA showed that using the nomogram model to predict the occurrence of CLNM risk would be better than using another two conditions (all patients and none of the patients treated). This means that the model is clinically useful when intervention is decided on in the range of the threshold probability between 0.09-0.82 and 0.07-0.86 in the training and validation groups respectively.

Novel risk stratification based on the predictive nomogram

Each variable contained in the nomogram has its corresponding risk point, and the total points calculated for all patients can quantitatively predict their respective CLNM risk. The distribution characteristic of the total CLNM risk points are shown in Figure 8, and the risk value is shown in Figure 4. We therefore determined three cut-off values (150, 200 and 240) by using recursive partition analysis, and classified three subgroups as follows: (1) extreme low-risk group (total points ≤ 150 , risk $\leq 18\%$), low-risk group ($151 \leq$ total points ≤ 200 , risk 19-36%), (2) moderate-risk group ($201 \leq$ total points ≤ 240 , risk 37-58%), (3) high-risk group (total points > 250 , risk $> 58\%$). In the training and validation groups, the rates of CLNM for extreme low-, low-, moderate-, and high-risk groups were 10.57%, 24.64%, 45.89%, 69.88% and 10.65%, 22.92%, 53.57%, 83.33%, respectively, showing a gradual upward trend. We further studied whether the relative risk of CLNM in low-, moderate-, and high-risk groups was significantly different from one another. The Chi-square test

showed that there were significant differences between all groups ($P < 0.05$). The results of the training and validation groups confirmed that there were no significant differences in the same category group ($P > 0.05$). As shown in Table 3.

Follow-up of postoperative serum thyroid function indicators

We retrospectively collected complete follow-up data on serum thyroid function indicators for 4 years after surgery in 789 patients with PTMC, of whom 158 (20.03%) developed CLNM and 631 (79.97%) did not, which was not statistically significant difference when compared with the overall distribution of CLNM occurrence ($\chi^2 = 0.068$, $P = 0.794$). The differences in FT3, TSH, and TPOAb in the preoperative CLNM (+) group were statistically significant compared with the CLNM (-) group, which were also previously screened by LASSO regression.

The follow-up data of serum thyroid function indicators in PTMC patients during 4 years after surgery and the results of comparison between CLNM (+) and CLNM (-) groups are shown in Table 4, Figure 9. FT3 decreased to the lowest value 3.28 ± 0.77 pmol/L at 3 days postoperatively, then gradually increased to a relatively stable state of 4.97 ± 0.97 pmol/L at 3 months postoperatively, and was significantly higher in the CLNM (+) group than in the CLNM (-) group ($P < 0.05$). FT4 remained elevated for 3 months postoperatively and then stabilized at 20.09 ± 4.44 pmol/L, which was higher than the preoperative level of 15.90 ± 2.52 pmol/L, the CLNM (+) group was higher than the CLNM (-) group ($P < 0.05$). The mean TSH level reached the highest value 6.84 ± 13.19 uIU/ml at 1 month postoperatively, then gradually decreased and was maintained at a stable level (2.36 ± 8.52 uIU/ml) at 3 months postoperatively, there

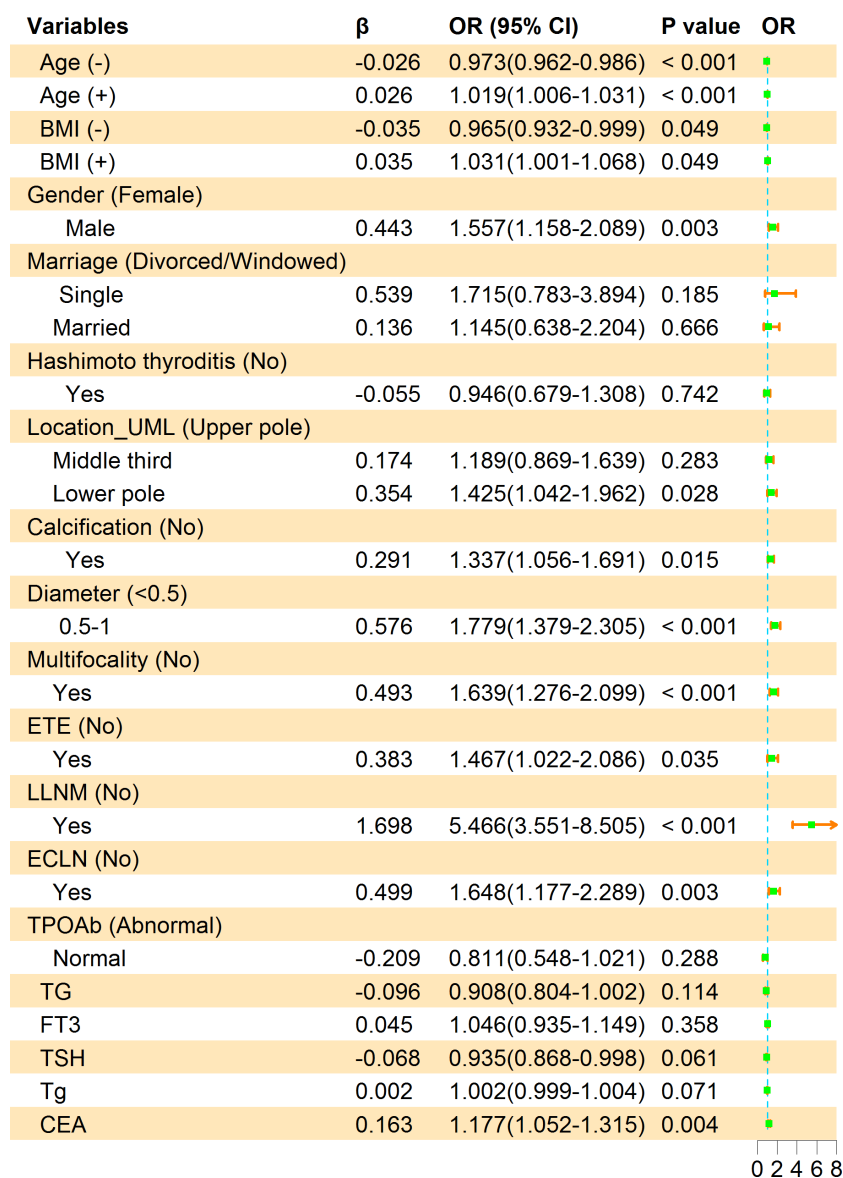


FIGURE 3 Multivariate logistic regression analysis of factors associated with CLNM in the training group. β is the regression coefficient; CI, confidence interval; OR, odds ratio. The symbols (+) indicate positive correlation and (-) represent negative correlation.

was no statistically significant difference between the CLNM (+) and CLNM (-) groups ($P > 0.05$). The mean Tg level reached a maximum value of 60.72 ± 93.59 ng/ml at 3 days postoperatively, then gradually decreased and remained at a stable level 4.00 ± 13.95 ng/ml at 1 month postoperatively, which was lower than the preoperative level of 21.65 ± 50.23 ng/ml, and the difference between the CLNM (+) and CLNM (-) groups was not statistically significant ($P > 0.05$). TGAb showed a gradual decrease, with no statistical difference between the CLNM (+) and CLNM (-) groups ($P > 0.05$). TPOAb also showed a gradual decline, with CLNM (+) group being lower than the CLNM (-) group, with a statistically significant difference within 1 year postoperatively ($P < 0.05$).

Thyroid function indicators FT3, FT4, and Tg varied within the normal range, TSH exceeded the maximum normal level at 1 month postoperatively, the CLNM (+) group with TGAb and the CLNM

(-) group with TPOAb exceeded the highest normal level within 6 months and then gradually decreased to the normal range.

The composition ratio of normal and abnormal reference ranges of serum thyroid function indicators during the 4 years postoperative follow-up in the CLNM (+) and CLNM (-) groups are shown in **Figure 10**. The proportions of $FT3 < 3.1$ pmol/L and $FT4 < 12$ pmol/L reached its maximum at 3 days postoperatively and were higher in the CLNM (+) group than in the CLNM (-) group, then gradually decreased to 0. $TSH > 4.2$ uIU/ml reached highest value at 1 month postoperatively, with 33.49% and 28.42% in the CLNM (+) and CLNM (-) groups, respectively, and then gradually declined. The proportion with $Tg < 3.5$ ng/ml increases dramatically at 1 month postoperatively. TGAb and TPOAb varied steadily, with an overall gradual decline in the portion above the normal range.

TABLE 2 Risk factors characteristics associated with CLNM in PTMC.

Variables	Training group n (%)			Validation group n (%)			Total n (%)		
	CLNM (+)	CLNM (-)	P value	CLNM (+)	CLNM (-)	P value	CLNM (+)	CLNM (-)	P value
Total	433 (100)	1683 (100)		188 (100)	719 (100)		621 (100)	2402 (100)	
Gender			< 0.001			0.004			< 0.001
Male	130 (30.02)	321 (19.07)		54 (28.72)	137 (19.05)		184 (29.63)	458 (19.07)	
Female	303 (69.98)	1362 (80.93)		134 (71.28)	582 (80.95)		437 (70.37)	1944 (80.93)	
Location_UML			0.029			0.033			0.001
Upper pole	79 (18.24)	378 (22.46)		30 (15.96)	165 (22.95)		109 (17.55)	543 (22.61)	
Middle third	167 (38.57)	687 (40.82)		74 (39.36)	298 (41.45)		241 (38.81)	985 (41.01)	
Lower pole	187 (43.19)	618(36.72)		84 (44.68)	256 (35.60)		271 (43.64)	874 (36.38)	
Calcification			< 0.001			0.044			< 0.001
No	245 (56.58)	1117 (66.37)		108 (57.45)	470 (65.37)		353 (56.84)	1587 (66.07)	
Yes	188 (43.42)	566 (33.63)		80 (42.55)	249 (34.63)		268 (43.16)	815 (33.93)	
Diameter			< 0.001			< 0.001			< 0.001
<0.5	112 (25.87)	766 (45.51)		30 (15.96)	351 (48.82)		142 (22.87)	1117 (46.50)	
0.5-1	321 (74.13)	917 (54.49)		158 (84.04)	368 (51.18)		479 (77.13)	1285 (53.50)	
Multifocality			< 0.001			< 0.001			< 0.001
No	273 (63.05)	1300 (77.24)		116 (61.70)	571 (79.42)		389 (62.64)	1871 (77.89)	
Yes	160 (36.95)	383 (22.76)		72 (38.30)	148 (20.58)		232 (37.36)	531 (22.11)	
ETE			< 0.001			< 0.001			< 0.001
No	361 (83.37)	1554 (92.33)		154 (81.91)	673 (93.60)		515 (82.93)	2227 (92.71)	
Yes	72 (16.63)	129 (7.67)		34(18.08)	46 (6.40)		106 (17.07)	175 (7.29)	
LLNM			< 0.001			< 0.001			< 0.001
No	360 (83.14)	1642 (97.56)		154 (81.91)	708 (98.47)		514 (82.77)	2350 (97.84)	
Yes	73 (16.86)	41 (2.44)		34 (18.09)	11 (1.53)		107 (17.23)	52 (2.16)	
ECLN			<0.001			0.006			<0.001
No	352 (81.29)	1530 (90.91)		151 (80.32)	633 (88.04)		503 (81.00)	2163 (90.05)	
Yes	81 (18.71)	153 (9.09)		37 (19.68)	86 (11.96)		118 (19.00)	239 (9.95)	
Age	44.44 ± 11.44	47.99 ± 10.04	<0.001	44.87 ± 10.42	48.14 ± 10.13	<0.001	44.57 ± 11.13	48.04 ± 10.06	<0.001
BMI	24.55 ± 3.59	24.94 ± 3.54	0.002	24.59 ± 3.66	24.93 ± 3.47	0.027	24.57 ± 3.61	24.94 ± 3.51	0.009
CEA	1.66 ± 1.09	1.51 ± 0.98	0.012	1.65 ± 1.40	1.56 ± 1.09	0.104	1.66 ± 1.19	1.53 ± 1.02	0.017

The incidences of subclinical hypothyroidism and hypothyroidism tended to increase and then decrease in both the CLNM (+) and CLNM (-) groups, as shown in Figures 11A, B. Subclinical hypothyroidism occurred predominantly within 6 months postoperatively and reached a maximum at 1 month postoperatively, with a higher incidence in the CLNM (+) group than in the CLNM (-) group, at 24.68% and 19.65%, respectively. The overall incidence were 42.41% (67 of 158 patients) in the CLNM (+) group and 42.31% (267 of 631 patients) in the CLNM (-) group. Hypothyroidism appeared mainly within 3 months postoperatively and peaked at 1 month postoperatively, with an incidence of 8.86% in the CLNM (+) group higher than that of

5.71% in the CLNM (-) group. The overall incidence were 16.46% (26 of 158 patients) in the CLNM (+) group and 12.04% (76 of 631 patients) in the CLNM (-) group.

Discussion

The incidence of thyroid cancer has risen rapidly in most parts of the world over the past 30 years, and more markedly in developed countries (20, 21). PTC is the most common type of differentiated thyroid malignancy and it represents about 90% of all thyroid cancers (22, 23). PTMC is a subtype of PTC, defined as PTC with

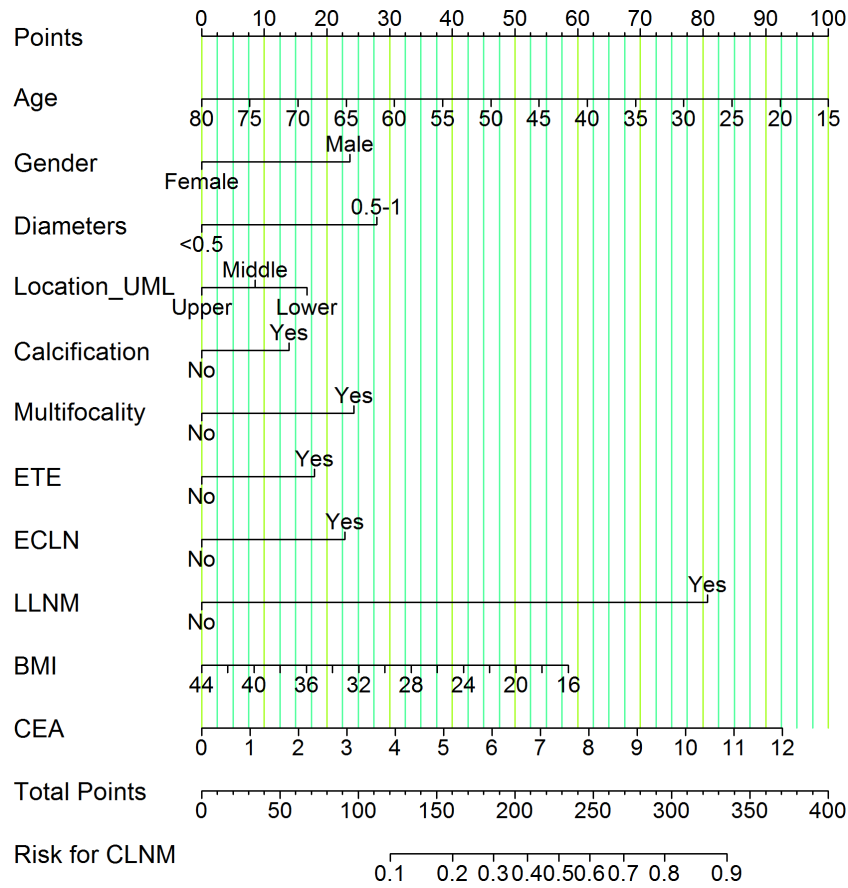


FIGURE 4

Nomogram of CLNM risk in patients with PTMC. We calculated the corresponding points according to the assigning principle. Gender: 23.75 points for male; Diameters: 28.00 points for 0.5-1 cm; Location_UML: 17.00 points for lower pole and 8.75 points for middle third; Calcification: 13.75 points for yes; Multifocality: 24.00 points for yes; ETE: 18.00 points for yes; ECLN: 22.50 points for yes; LLNM: 81.00 points for yes; Age: point range is 0-100, with an increase of 1.54 points for each additional year of age. BMI: Based on a scale of 0-58.50, 2.09 points are added to the score for every 1 kg/m² reduction in BMI. CEA: on a scale from 0 to 92.50, each 1 ng/mL raise in CEA is associated with an increase of 7.71 points. Each risk factor score add up to the total points, which represents the risk for CLNM.

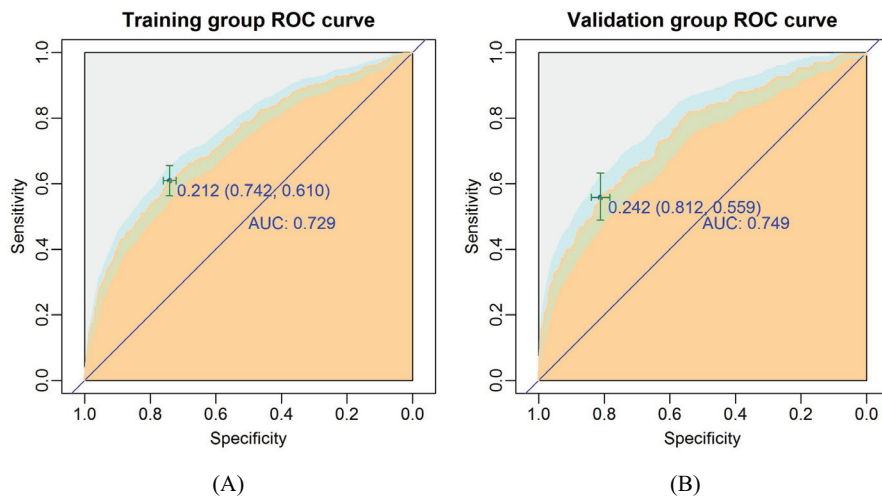


FIGURE 5

The ROC curves of the nomogram for CLNM risk. (A) Training group; (B) Validation group. The burly wood color represents the area under the ROC curve; 95% CI of the ROC curve was colored light blue.

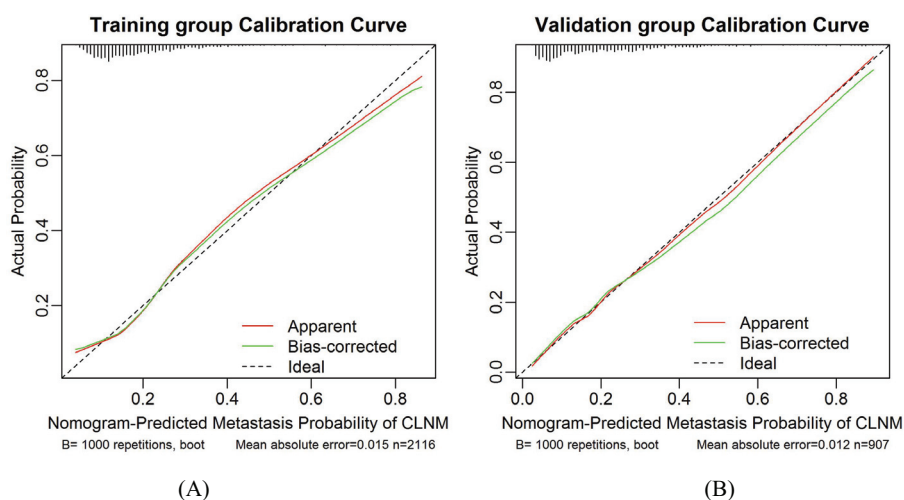


FIGURE 6 Calibration curves for the training group and validation group models. (A) Training group. (B) Validation group. The diagonal dotted line represents the ideal prediction by the perfect nomogram. The green solid line represents the performance of the nomogram. The closer the green solid line is to the diagonal dotted line, the stronger the predictive ability of the model. The red solid line indicates the apparent predictive accuracy.

tumors up to 10 mm in maximum diameter (5). The number of PTMC patients is increasing due to the use of high-resolution ultrasound (USG) and fine needle biopsy (24). Although in the majority of patients PTMC is usually associated with a good prognosis, PTMC with CLNM is not uncommon. In addition, several studies have demonstrated lymph node metastases at presentation, with locoregional recurrence during the follow-up period (25, 26). Some researchers recommend the use of prophylactic CLND in patients with PTMC (27, 28), but this approach remains a matter of debate. Therefore, determining the predictors of CLNM is very important to avoid unnecessary CLND in patients with PTMC. To improve the diagnostic accuracy of PTMC, many authors have used a combination of clinicopathological and USG features (29). High-resolution

ultrasonography is helpful in evaluating LNM (30). However, despite the high diagnostic accuracy in detecting the LLNM, the accuracy of ultrasonography in preoperative detection of CLNM is limited (31). Consequently, preoperative assessment of CLNM in PTMC patients is challenging. Thus, a tool that helps to quantify the risk of nodal metastasis may facilitate preoperative decision-making (32). For these reasons, several authors have developed different predictive models to assess the risk of CLNM in patients with PTMC that combine clinical, analytical, and ultrasound variables (18, 32). These may help clinicians and patients improve clinical decision-making.

Nomograms are statistical tools that are ideally suited to individualizing risk assessment and they have been used for a variety of situations (33). Nomograms have been shown to

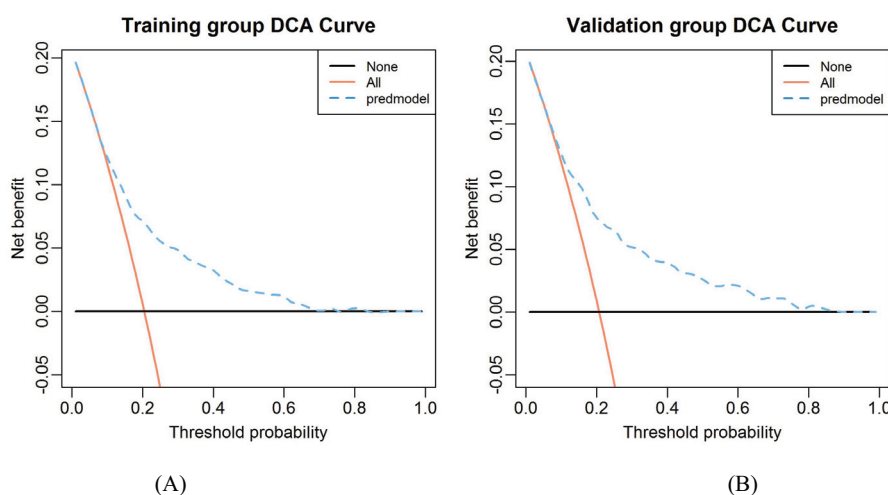


FIGURE 7 The decision curve analysis for CLNM in the constructed risk nomogram. (A) Training group. (B) Validation group.

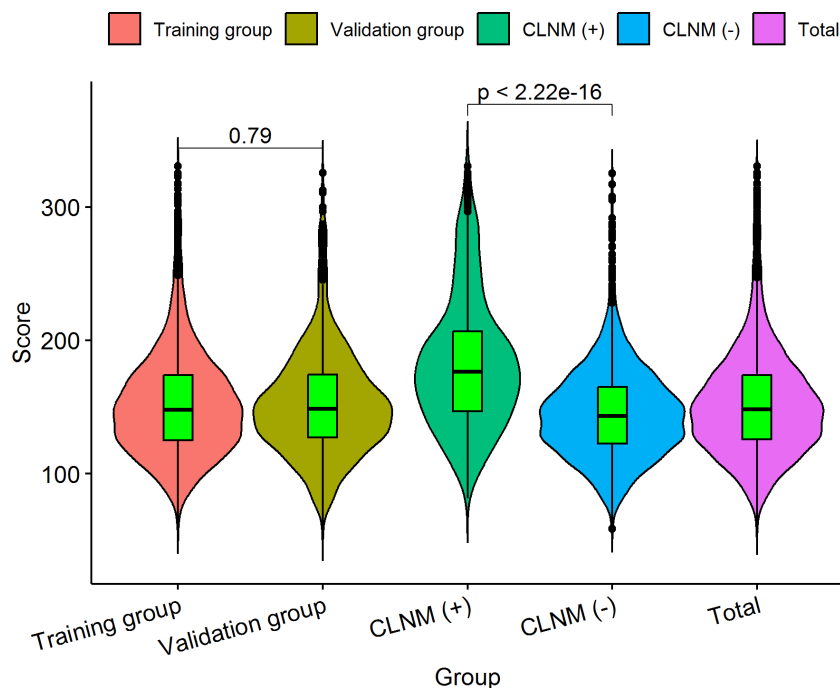


FIGURE 8

The distribution characteristic of the total CLNM risk points. The length of the violin chart represents the range of points, the width indicates the frequency of points, and the black horizontal line in the boxplot represents the average points. We calculated that the average points of the training group is 153.22 ± 41.11 (61.12-330.68), and 152.92 ± 40.07 (58.80-325.38) for the validation group; there was no significant difference ($P = 0.790$) between the two groups. The average points of the CLNM (+) group 182.73 ± 49.72 (81.60-330.68) was significantly higher than that of CLNM (-) group 145.48 ± 34.22 (58.80-325.19), with a statistically significant difference ($P < 0.001$).

outperform even recognized by experts in the field of oncology (34, 35). In this study, we included the clinical characteristics, biochemical profiles, ultrasonographic and cytologic features in a nomogram and predicted the risk of CLNM in patients with PTMC. The original data were randomly divided into a training group (model construction) and a validation group (model validation), the verification results showed that both have good risk prediction ability. The model was assessed to have good discrimination and calibration capabilities by plotting ROC curves and calibration

curves. Meanwhile, DCA also confirmed the clinical utility value of the nomogram. This study suggested that age, gender, calcification, diameter, multifocality, ETE, ECLN, LLNM, location_UML, BMI, and CEA were independent risk factors for CLNM in patients with PTMC. Among them, male gender, $1 \geq$ diameter $\geq 0.5\text{cm}$, calcification, multifocality, ETE, LLNM, ECLN, location in lower pole and CEA correlated positively with CLNM. Age and BMI correlated negatively with CLNM. LLNM was the most strongly correlated indicator. The nomogram we constructed

TABLE 3 Metastasis risk stratification of patients with PTMC based on risk scores of the nomogram model.

Nomogram	ELR	LR	MR	HR	Total	P value	ELR-LR	ELR-MR	ELR-HR	LR-MR	LR-HR	MR-HR
	≤ 150	151-200	201-240	≥ 241			P value	P value	P value	P value	P value	P value
Training group												
CLNM (+)	118 (10.57)	190 (24.64)	67 (45.89)	58 (69.88)	433	< 0.001	< 0.001	< 0.001	< 0.001	< 0.001	< 0.001	< 0.001
CLNM (-)	998 (89.43)	581 (75.36)	79 (54.10)	25 (30.12)	1683							
Total	1116	771	146	83	2116							
Validation group												
CLNM (+)	51 (10.65)	77 (22.92)	30 (53.57)	30 (83.33)	188	< 0.001	< 0.001	< 0.001	< 0.001	< 0.001	< 0.001	0.003
CLNM (-)	428 (89.35)	259 (77.08)	26 (46.43)	6 (16.67)	719							
Total	479	336	56	36	907							
P value	0.965	0.537	0.328	0.125								

ELR, extreme low risk; LR, low risk; MR, moderated risk; HR, high risk.

TABLE 4 4-year follow-up results of thyroid function in the CLNM (+) and CLNM (-) groups of PTMC patients.

Variables	Time	Total n = 789	CLNM (+) n = 158	CLNM (-) n = 631	t	P
FT3						
	Preoperative	4.65 ± 0.76	4.77 ± 0.92	4.61 ± 0.72	-2.613	0.009
	3 days	3.28 ± 0.77	3.23 ± 0.82	3.29 ± 0.76	1.029	0.304
	1 month	4.49 ± 0.91	4.50 ± 0.91	4.49 ± 0.91	-0.060	0.953
	3 months	4.97 ± 0.97	5.17 ± 1.06	4.92 ± 0.94	-2.898	0.004
	6 months	4.89 ± 0.89	5.17 ± 0.88	4.82 ± 0.88	-4.113	<0.001
	1 year	4.70 ± 0.81	4.95 ± 0.92	4.64 ± 0.77	-3.966	<0.001
	2 years	4.66 ± 0.90	4.81 ± 0.84	4.62 ± 0.91	-1.774	0.077
	3 years	4.60 ± 0.76	4.85 ± 0.81	4.53 ± 0.73	-3.073	0.002
	4 years	4.89 ± 0.83	5.14 ± 0.64	4.82 ± 0.87	-2.444	0.015
FT4						
	Preoperative	15.90 ± 2.52	16.07 ± 2.79	15.85 ± 2.45	-0.999	0.319
	3 days	16.21 ± 3.95	15.62 ± 4.20	16.35 ± 3.87	2.319	0.021
	1 month	17.47 ± 4.27	17.14 ± 4.33	17.56 ± 4.25	1.216	0.224
	3 months	20.09 ± 4.44	21.23 ± 4.64	19.80 ± 4.34	-3.634	<0.001
	6 months	20.50 ± 4.46	21.67 ± 5.11	20.21 ± 4.23	-3.098	0.002
	1 year	20.13 ± 4.07	21.35 ± 4.92	19.84 ± 3.78	-3.193	0.002
	2 years	19.75 ± 3.70	20.92 ± 4.33	19.47 ± 3.47	-2.997	0.003
	3 years	19.47 ± 3.78	20.37 ± 4.25	19.24 ± 3.62	-2.153	0.032
	4 years	19.71 ± 3.67	21.41 ± 3.74	19.23 ± 3.53	-2.281	0.025
TSH						
	Preoperative	2.63 ± 1.60	2.41 ± 1.46	2.71 ± 1.63	2.366	0.018
	3 days	2.68 ± 3.20	3.06 ± 3.65	2.59 ± 3.07	-1.676	0.095
	1 month	6.84 ± 13.19	8.84 ± 17.05	6.33 ± 11.98	-1.946	0.053
	3 months	2.36 ± 8.52	1.66 ± 3.21	2.54 ± 9.38	1.947	0.052
	6 months	1.65 ± 7.13	1.54 ± 7.40	1.68 ± 7.07	0.215	0.829
	1 year	1.49 ± 6.96	1.63 ± 9.32	1.45 ± 6.26	-0.200	0.842
	2 years	1.01 ± 2.68	0.84 ± 1.48	1.05 ± 2.90	0.667	0.505
	3 years	1.44 ± 3.42	1.46 ± 4.17	1.43 ± 3.21	-0.072	0.943
	4 years	1.41 ± 3.46	0.50 ± 0.69	1.67 ± 3.87	1.268	0.208
Tg						
	Preoperative	21.65 ± 50.23	23.53 ± 50.24	21.17 ± 50.25	-0.587	0.557
	3 days	60.72 ± 93.59	51.67 ± 85.14	63.02 ± 95.55	1.520	0.129
	1 month	4.00 ± 13.95	5.40 ± 22.09	3.65 ± 10.95	-1.081	0.281
	3 months	3.48 ± 11.16	3.18 ± 17.05	3.55 ± 9.13	0.377	0.706
	6 months	2.97 ± 7.49	2.59 ± 11.39	3.06 ± 6.15	0.659	0.510
	1 year	2.48 ± 5.94	1.89 ± 5.94	2.62 ± 5.93	1.231	0.219
	2 years	1.84 ± 3.83	1.39 ± 3.75	1.95 ± 3.85	1.241	0.215
	3 years	1.68 ± 3.59	1.61 ± 4.55	1.70 ± 3.31	0.185	0.854

(Continued)

TABLE 4 Continued

Variables	Time	Total n = 789	CLNM (+) n = 158	CLNM (-) n = 631	t	P
Tg						
	4 years	1.62 ± 4.37	2.81 ± 8.03	1.28 ± 2.54	-0.794	0.437
TGAb						
	Preoperative	112.36 ± 366.07	154.76 ± 516.55	101.57 ± 316.11	-1.381	0.169
	3 days	83.52 ± 287.12	124.43 ± 437.55	72.94 ± 232.27	-1.545	0.124
	1 month	110.75 ± 333.02	135.69 ± 473.19	104.43 ± 287.07	-0.799	0.425
	3 months	95.69 ± 311.07	130.47 ± 522.49	87.36 ± 233.66	-0.912	0.363
	6 months	85.68 ± 282.86	118.39 ± 482.41	77.46 ± 204.41	-0.846	0.399
	1 year	75.82 ± 254.62	99.54 ± 385.92	69.81 ± 209.00	-0.751	0.454
	2 years	62.50 ± 220.99	89.07 ± 325.64	56.19 ± 188.03	-0.819	0.415
	3 years	45.00 ± 110.47	51.17 ± 116.20	43.44 ± 109.23	-0.441	0.659
	4 years	40.01 ± 74.23	42.23 ± 75.33	39.31 ± 74.74	-0.127	0.899
TPOAb						
	Preoperative	45.61 ± 98.53	30.84 ± 65.06	49.37 ± 105.07	3.099	0.002
	3 days	40.27 ± 91.03	26.87 ± 53.40	43.74 ± 98.18	3.139	0.001
	1 month	37.54 ± 77.43	25.78 ± 52.07	40.51 ± 82.39	2.800	0.005
	3 months	34.78 ± 71.25	24.89 ± 51.30	37.16 ± 75.09	2.199	0.029
	6 months	33.62 ± 71.60	23.31 ± 44.61	36.21 ± 76.72	2.234	0.026
	1 year	29.27 ± 62.81	20.50 ± 45.95	3 1.52 ± 66.29	1.966	0.051
	2 years	27.39 ± 60.48	22.63 ± 46.08	28.53 ± 63.43	0.738	0.461
	3 years	24.99 ± 53.69	12.54 ± 8.85	28.12 ± 59.52	3.541	<0.001
	4 years	22.58 ± 29.67	16.95 ± 20.23	24.37 ± 32.08	0.842	0.403

can well predict the risk of CLNM in patients with PTMC, which helps clinicians make decisions regarding the extent of surgical resection.

The AUC value is an important criterion for evaluating the performance of a model and is mainly used to demonstrate the discriminatory ability of the model. Yang et al. (36) established a nomogram to predict CLNM in PTMC patients with an AUC = 0.69, but there existed deficiencies in the study, for example, the small sample (291 PTMC patients) and the absence of validation. Wang et al. (37) estimated in a large retrospective study that the AUC of the nomogram predicting the risk of CLNM in patients with PTMC was 0.711. In our study, the AUC were 0.73, and 0.75 in the training and validation groups, respectively. Our estimated AUC values are significantly higher than the findings of some scholars, which fully demonstrates the good discriminatory ability of our constructed nomogram in detecting CLNM in patients with PTMC. It is worth mentioning that the AUC value of the constructed nomogram model in the validation group was 0.02 higher than that in the training group, which indicates that the model has better predictive performance in the validation group than in the training group, suggesting that the model is not overfitted, has some generalization ability, and can be better used in the dataset to predict the risk of

CLNM in patients with PTMC. However, the results of this study also have the limitation that the AUC value did not exceed 0.80, which suggests that the model we constructed could further improve its prediction performance, such as by adding gene mutation analysis, and by combining with future biological assessments including liquid biopsies and other possible risk factors.

Among the independent risk factors in this CLNM prediction model, LLNM was the factor with the greatest risk weight (OR = 5.43). Our findings is similar to those of Wang et al. (37). Therefore, when LLNM is detected during thyroid surgery, surgeons need to pay more attention to the central lymph nodes and evaluate the presence of CLNM. For patients with PTMC, tumor size was positively correlated with the risk of CLNM, the greater the diameter of the cancer lesion, the higher the risk and the worse the prognosis. However, the existing studies have no unified standard for the diagnostic cut-off value of cancer lesion size (37–39). Wang et al. (37) found that tumor size 0.5–1.0 cm was an independent predictor of central CLNM. Sun et al. (38) believed that PTMC patients with tumor diameter > 6 mm have higher rates of CLNM compared with patients with a tumor diameter ≤ 6 mm. Lim et al. (39) suggested that a nodule of 7 mm in size should be chosen as the diagnostic cut-off value. Our study also concluded that a diameter ≥ 0.5 cm is the threshold for CLNM, and logistic

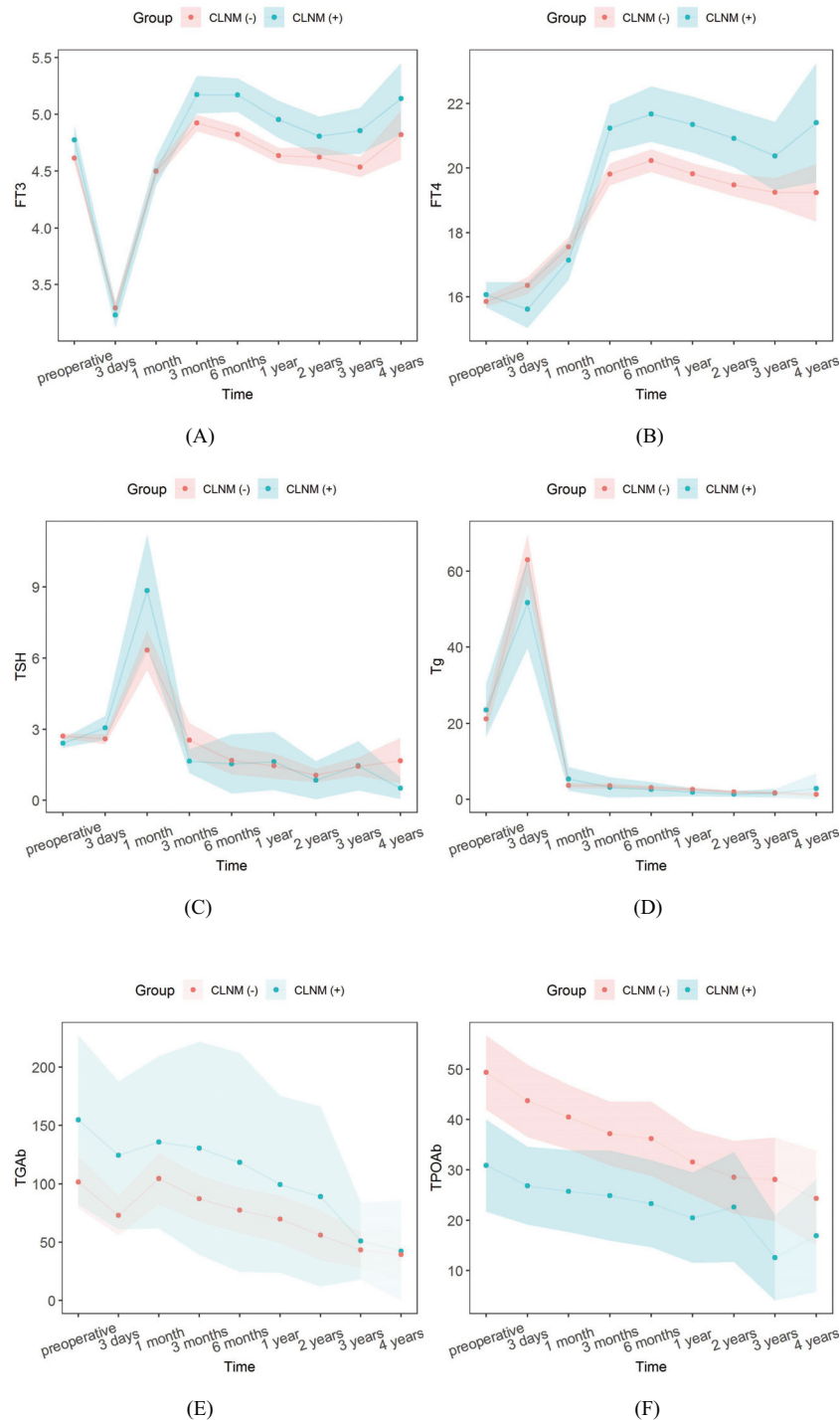


FIGURE 9 Trends in thyroid function outcomes of PTMC patients in the CLNM (+) and CLNM (-) group within 4 years follow-up. (A) FT3, (B) FT4, (C) TSH, (D) Tg, (E) TGAb, and (F) TPOAb.

multivariate regression analysis produces meaningful results (OR = 1.78). Multifocality was previously found to be associated with LNM in the central or lateral compartment (40). Multifocality is an indicator of the aggressiveness of PTC tumors, showing a higher tendency for regional LNM (41). Consistently, in our results on PTMC, multifocality was a higher risk factor for CLNM (OR = 1.66). Therefore, multifocality may be associated with the state of disease

progression, including risk stratification, management guidelines, and post-treatment monitoring in patients with PTMC. ETE has been recognized as an important prognostic factor in PTC (10, 35). ETE indicates poor prognosis for patients with PTC. However, the relationship between ETE and LNM has been examined in relatively small retrospective cohort studies (42, 43). As indicated in the study by Zhang et al. (44) and Sun et al. (38), ETE was a potential predictor for

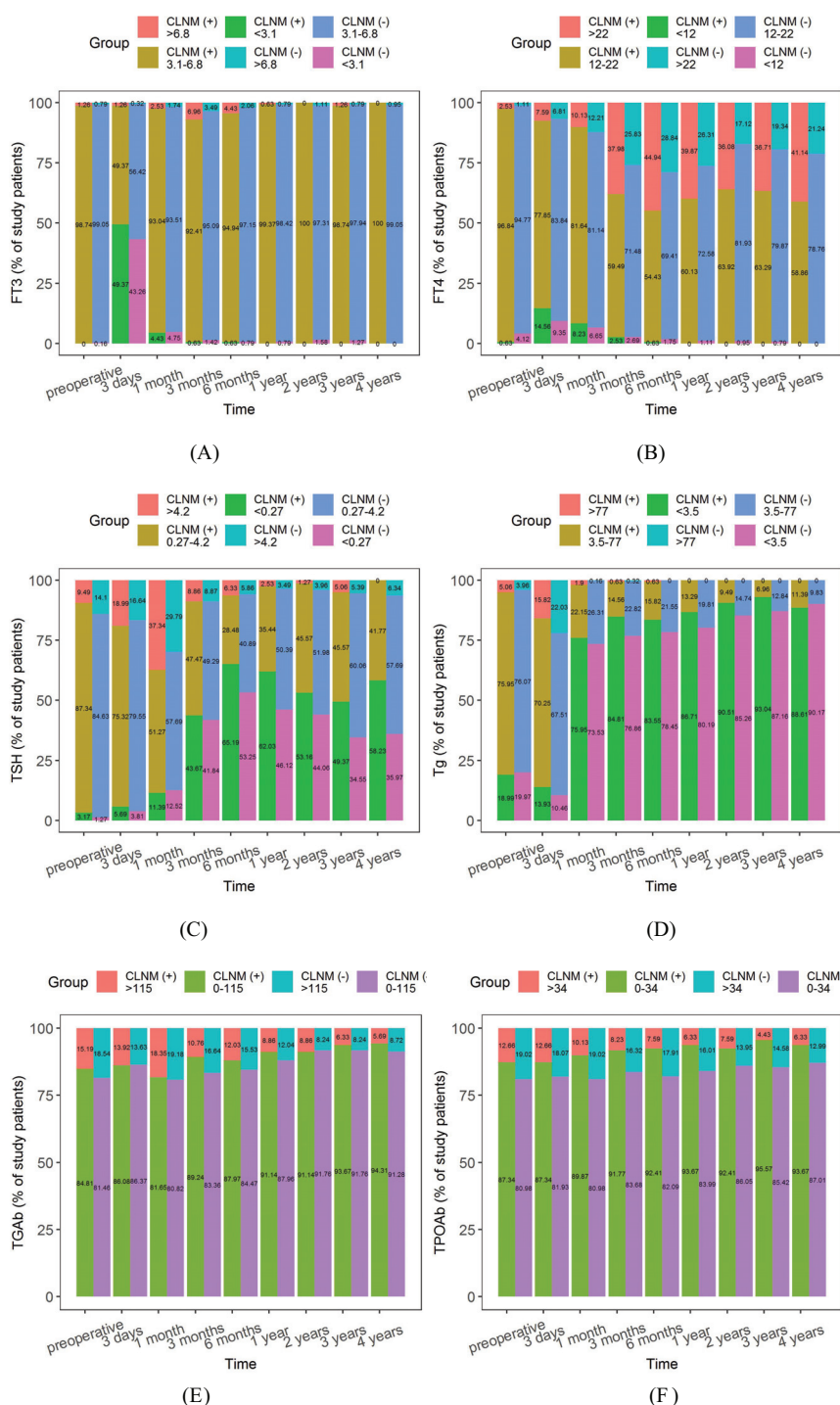


FIGURE 10

Composition ratio of normal and abnormal reference ranges of postoperative thyroid function indicators in the CLNM (+) and CLNM (-) groups of PTMC patients with 4 years follow-up. (A) FT3, (B) FT4, (C) TSH, (D) Tg, (E) TGAb, and (F) TPOAb.

CLNM in patients with PTMC. Our findings approximated theirs (OR = 1.47). The above risk factors were primarily derived from pathologic testing of patients with PTMC.

Our study showed that ultrasound findings of ECLN, tumors located at the lower pole, and calcification were also high risk factors for developing CLNM. The findings of Mohamed et al. (45) showed

that the presence of ECLN increased the predictive value of diagnosing PTC and suspicious thyroid nodules. The presence of an ECLN on the preoperative neck USG can provide valuable information to help surgeons determine the optimal surgical treatment for patients with suspected thyroid nodules (46). Our study also confirmed that ECLN is an independent risk factor for

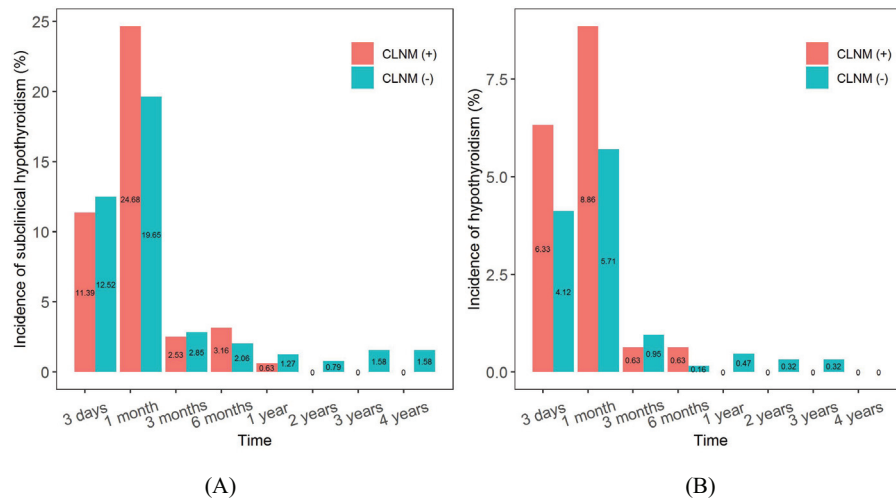


FIGURE 11

Incidences of subclinical hypothyroidism and hypothyroidism after surgery in the CLNM (+) and CLNM (-) groups of PTMC patients with 4-year follow-up. (A) subclinical hypothyroidism, (B) hypothyroidism.

CLNM (OR = 1.66). We believe that the above studies will encourage further research investigating the association between ECLN and CLNM in patients with PTMC. Zhang et al. (47) hypothesized that the risk of LNM for PTC nodules at different locations might be associated with blood reflux. PTC cells in the upper region are more likely to transport to the lateral lymph nodes through the lymph flow along the superior thyroid artery (48). Hence, tumors located in the upper thyroid lobe confer a lower risk of developing CLNM, and conversely, tumors located in the lower thyroid lobe confer a high risk of developing CLNM (49, 50). Calcification is an important ultrasound feature of PTC (51). Microcalcifications are considered to be the most specific sonographic indicator in the diagnosis of PTC (52, 53). In this study, we found that calcification on the USG image is a risk factor for CLNM (OR = 1.34). Calcification is a calcium salt deposition caused by the proliferation of blood vessels and fibers, reflecting the rapid growth of cancer cells. Therefore, if calcifications are found in the nodules, the lymph node status in the central region should be assessed more carefully.

Among the biochemical variables and basic patient information, the male gender, CEA, young age and lower BMI are also independent risk factors of CLNM in patients with PTMC. It was confirmed in the study by Li et al. (54) that males had higher average annual percentage changes in thyroid cancer incidence and mortality rates than females. There are several explanations for these differences between males and females. Firstly, women undergo thyroid tests more frequently, and they are more likely to participate in medical treatment. Furthermore, this difference may be due to physiological differences between males and females (55, 56). In agreement with results of several previous studies (9, 57), male gender (OR = 1.60) was found to be an independent predictor for CLNM in PTMC. CEA is a broad spectrum tumor marker that has been found to be elevated in some patients with PTC (58). For example, Yan et al. (59) indicated that the combination of serum CEA, Tg, and CK 18 significantly improved the diagnostic efficiency of PTC patients. A retrospective cohort study of two clinical centers showed that CEA > 1

ng/mL was significantly associated with CLNM (18). Our research also confirmed that patients in CLNM (+) group had higher levels of CEA (1.66 ± 1.19 ng/ml) than those in the CLNM (-) group (1.53 ± 1.02 ng/ml) and the difference was statistically significant ($P = 0.017$), and the probability density distribution of CEA is shown in Figure 12A. Age is a well-established prognostic factor for thyroid cancer survival, and it is included in the American Joint Committee on Cancer (AJCC) thyroid cancer-staging system (59, 60). Ito et al. (61) reported that being young was an independent predictor of progression in PTMC under observation, including novel LNM. Our study also suggested that younger people were more likely to develop CLNM, and the age of the CLNM (+) group (44.57 ± 11.13 years) was lower than that of the CLNM (-) group (48.04 ± 10.06 years), with a statistically significant difference ($P < 0.001$), and the probability density distribution of the age is shown in Figure 12B. However, we did not stratify for age, which still needs to be investigated in studies with larger sample sizes. Our nomogram model quantitatively showed that patients with low BMI had a higher risk of developing CLNM, with a lower BMI in the CLNM (+) group (24.57 ± 3.61 kg/m²) than in the CLNM(-) group (24.94 ± 3.51 kg/m²), the difference was statistically significant ($P = 0.009$), and the probability density distribution of BMI are shown in Figure 12C. The results were consistent with Zhao et al. (62). Of course, some scholars have suggested that BMI is positively associated with CLNM (63). But the sample size of our study was larger than theirs. This finding may be due to the small sample size in multivariate analysis of potential comprehensive risk factors in real clinical scenarios, which may lead to bias in individual factors. To address this issue, we will continue to expand the sample size and conduct multi-center studies to further validate these results.

Currently, studies on the follow-up of thyroid function after thyroid cancer surgery have been reported, some of which explored the incidence, risk factors, and clinical features of hypothyroidism after thyroid cancer resection, but did not analyze in depth the differences in thyroid function between the CLNM (+) and CLNM (-) groups. In this study, we systematically analyzed trends

in complete indicators of thyroid function in the CLNM (+) and CLNM (-) groups in 789 postoperative thyroid cancer patients followed for 4 years. Bae et al. (19) analyzed thyroid function in 369 postoperative thyroid cancer patients follow-up for 2 years and demonstrated that TSH concentration gradually increased over 3-6 months and then decreased to a level higher than preoperative level, whereas FT4 concentration showed opposite trend in consecutive measurements. In our study, the overall trend of TSH and FT4 levels were almost identical to their results. Postoperative changes in FT4 and TSH levels affect the incidence of postoperative complications subclinical hypothyroidism and hypothyroidism.

Hypothyroidism after thyroid cancer resection is a major clinical problem, as a significant number of patients require thyroid hormone replacement therapy. Verloop et al. (64) reported through a systematic review that the overall risk of hypothyroidism after lobectomy was 22% (range 7-49%). Studies by Ahn et al. (65) and Park et al. (66) illustrated that the incidence of subclinical hypothyroidism after hemithyroidectomy was as high as 55.8% and 64.2%, respectively. Subclinical hypothyroidism developed in the early postoperative period (1-3 months postoperatively) in most cases (84.5%). Our

research showed that the incidence of subclinical hypothyroidism and hypothyroidism was significantly higher in the CLNM (+) group than in the CLNM (-) group at 1 month postoperatively, after which the incidence in the CLNM (+) group decreased dramatically to zero. The overall incidence of hypothyroidism was 18.35% in the CLNM (+) group and 13.79% in the CLNM (-) group. The results suggested that our findings are within the range of Verloop et al. (64), indicating that they are reasonable. We analyzed the differences in thyroid function between the CLNM (+) and CLNM (-) groups, which were mainly attributed to the extent of surgical removal of the thyroid gland, comparative results after total thyroidectomy and hemithyroidectomy are presented in the [Supplementary Table S1](#), [Supplementary Figures S1, S2](#). The proportions of patients who underwent total thyroidectomy in the CLNM (+) and CLNM (-) groups were 63.92% (101 out of 158 patients) and 43.58% (275 out of 631 patients), respectively, which implied that patients in the CLNM (+) group were more prone to thyroid dysfunction in the postoperative period, and required levothyroxine supplementation to regulate the thyroid hormone levels.

Postoperative complications of PTMC also include laryngeal nerve palsy, hypoparathyroidism, blood loss, hematoma, and

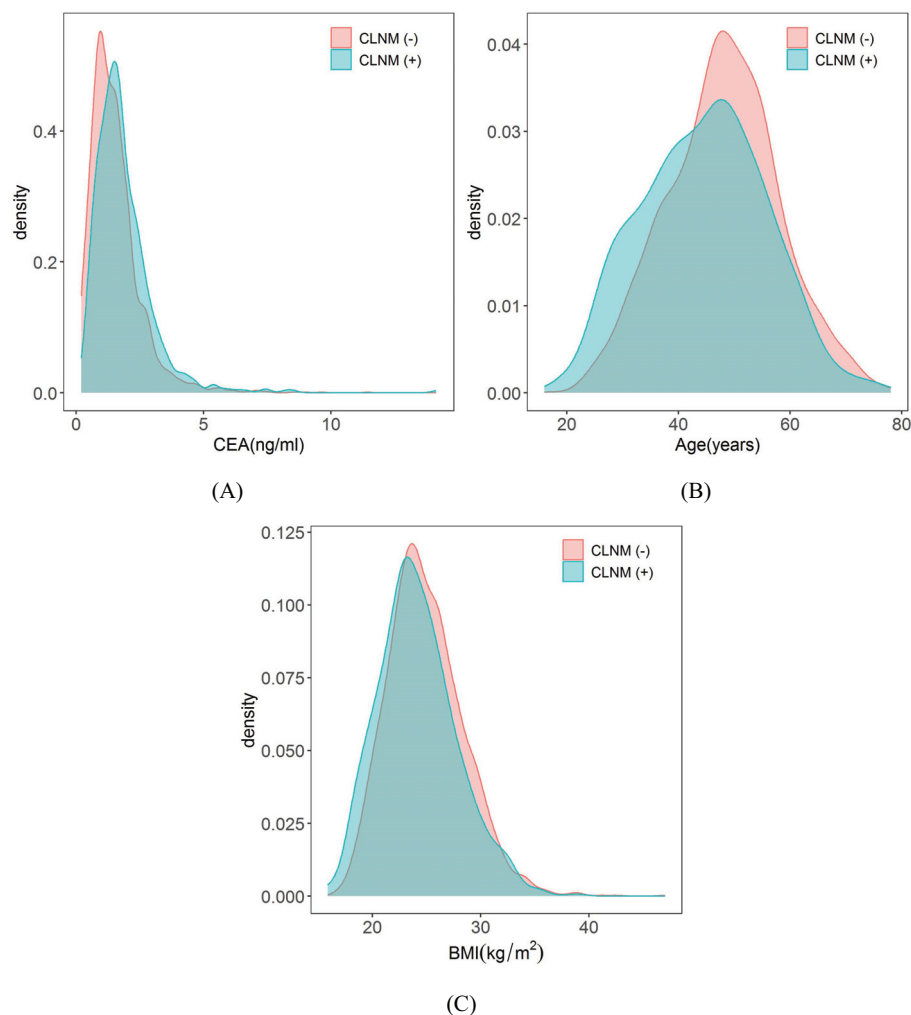


FIGURE 12

Probability density distribution of CEA, Age and BMI in CLNM (+) group and CLNM (-) group respectively. (A) CEA, (B) Age, and (C) BMI.

wound infection, which were not comprehensively analyzed in this study and were only associated with subclinical hypothyroidism and hypothyroidism that can be calculated by follow-up thyroid function indicators. However, Ultrasonic scalpel and the Ligasure have been proven to be safe, effective, useful, and time-saving as alternatives to the traditional surgical thyroid suture ligation techniques. They simplify total thyroidectomy, eliminating the need for clamp-and-tie maneuvers and achieving efficient hemostasis (67, 68). This means a shorter operation time and a lower postoperative complication rate. Relevant studies will be further analyzed in a comprehensive and systematic manner.

In this study, the nomogram model based on clinical, biochemical, ultrasound and pathological features had good predictive performance. Meanwhile, the calibration plots and DCA results also proved that the prediction model has good discriminatory ability and clinical application value. The present study still has the following deficiencies: (1) The internal validation of the nomograms in this study came from the same hospital and lacked external validation, which may have resulted in case selection bias. Therefore, further analysis and evaluation should be carried out in combination with multicenter large-sample clinical data. (2) A larger sample size of clinical data is still needed to improve the validity and reliability of the model. (3) Some data in this study need further stratification and quantitative research. (4) Lastly, our study is retrospective, and prospective studies in larger patient populations are required to identify and validate this risk prediction model to improve clinical management.

Conclusion

Accurate preoperative identification of CLNM is essential for surgical protocol establishment for patients with PTMC. Therefore, it is necessary to search for risk factors for CLNM in PTMC patients. In this study, we proposed a nomogram model combining clinical, biochemical, ultrasound and pathological features. With the visualization of a nomogram model, it may help clinical practitioners inform screening and early diagnosis of CLNM by incorporating patient information into risk prediction models and calculating risk scores to assess the risk of CLNM in patients with PTMC. Regular follow-up of postoperative thyroid function indicators and the incidence of complications in PTMC patients can provide clinicians with a reference for developing postoperative treatment plans.

Data availability statement

The raw data supporting the conclusions of this article will be made available by the authors, without undue reservation.

Ethics statement

The studies involving humans were approved by The Medical Ethics Committee of Traditional Chinese Medicine Hospital

Affiliated to Xinjiang Medical University. The studies were conducted in accordance with the local legislation and institutional requirements. The participants provided their written informed consent to participate in this study.

Author contributions

YH: Writing – original draft, Validation, Resources, Formal analysis, Data curation, Conceptualization. PL: Writing – original draft, Visualization, Software, Methodology, Formal analysis, Data curation. HL: Writing – original draft, Investigation, Conceptualization. YL: Writing – original draft, Validation, Investigation. LM: Writing – review & editing, Validation, Supervision, Resources, Investigation. KW: Writing – review & editing, Visualization, Supervision, Software, Project administration, Methodology, Funding acquisition, Formal analysis.

Funding

The author(s) declare financial support was received for the research, authorship, and/or publication of this article. This research was funded by the Key R&D Program of Xinjiang Uygur Autonomous Region (2023B03002), major science and technology projects of Xinjiang Autonomous Region (2022A03019-1), and the 14-th Five-Year Plan Distinctive Program of Public Health and Preventive Medicine in Higher Education Institutions of Xinjiang Uygur Autonomous Region.

Conflict of interest

The authors declare that the research was conducted in the absence of any commercial or financial relationships that could be construed as a potential conflict of interest.

Publisher's note

All claims expressed in this article are solely those of the authors and do not necessarily represent those of their affiliated organizations, or those of the publisher, the editors and the reviewers. Any product that may be evaluated in this article, or claim that may be made by its manufacturer, is not guaranteed or endorsed by the publisher.

Supplementary material

The Supplementary Material for this article can be found online at: <https://www.frontiersin.org/articles/10.3389/fendo.2024.1395900/full#supplementary-material>

References

- Li F, Chen G, Sheng C, Gusdon AM, Huang Y, Lv Z, et al. BRAFV600E mutation in papillary thyroid microcarcinoma: a meta-analysis. *Endocr Relat Cancer*. (2015) 22:159–68. doi: 10.1530/ERC-14-0531
- Wang K, Xu J, Li S, Liu S, Zhang L. Population-based study evaluating and predicting the probability of death resulting from thyroid cancer among patients with papillary thyroid microcarcinoma. *Cancer Med*. (2019) 8:6977–85. doi: 10.1002/cam4.2597
- Shi Y, Yang Z, Heng Y, Ju H, Pan Y, Zhang Y. Clinicopathological findings associated with cervical lymph node metastasis in papillary thyroid microcarcinoma: A retrospective study in China. *Cancer Control*. (2022) 29:10732748221084926. doi: 10.1177/10732748221084926
- Siegel RL, Miller KD, Jemal A. Cancer statistics, 2020. *CA Cancer J Clin*. (2020) 70:7–30. doi: 10.3322/caac.21590
- Baloch ZW, Asa SL, Barletta JA, Ghossein RA, Juhlin CC, Jung CK, et al. Overview of the 2022 WHO classification of thyroid neoplasms. *Endocr Pathol*. (2022) 33:27–63. doi: 10.1007/s12022-022-09707-3
- Hay ID, Hutchinson ME, Gonzalez-Losada T, McIver B, Reinalda ME, Grant CS, et al. Papillary thyroid microcarcinoma: a study of 900 cases observed in a 60-year period. *Surgery*. (2008) 144:980–7. doi: 10.1016/j.surg.2008.08.035
- Lee KJ, Cho YJ, Kim SJ, Lee SC, Kim JG, Ahn CJ, et al. Analysis of the clinicopathologic features of papillary thyroid microcarcinoma based on 7-mm tumor size. *World J Surg*. (2011) 35:318–23. doi: 10.1007/s00268-010-0886-5
- Ito Y, Uruno T, Nakano K, Takamura Y, Miya A, Kobayashi K, et al. An observation trial without surgical treatment in patients with papillary microcarcinoma of the thyroid. *Thyroid*. (2003) 13:381–7. doi: 10.1089/105072503321669875
- Qu N, Zhang L, Ji QH, Chen JY, Zhu YX, Cao YM, et al. Risk factors for central compartment lymph node metastasis in papillary thyroid microcarcinoma: A meta-analysis. *World J Surg*. (2015) 39:2459–70. doi: 10.1007/s00268-015-3108-3
- Haugen BR, Alexander EK, Bible KC, Doherty GM, Mandel SJ, Nikiforov YE, et al. American thyroid association management guidelines for adult patients with thyroid nodules and differentiated thyroid cancer: the american thyroid association guidelines task force on thyroid nodules and differentiated thyroid cancer. *Thyroid*. (2015) 26:1–133. doi: 10.1089/thy.2015.0020
- Xiang T, Yan W, Zhou L. Retrospective analysis of prognostic factors in patients of papillary thyroid microcarcinoma. *Oncotarget*. (2018) 9:35553–8. doi: 10.18632/oncotarget.26248
- Takami H, Ito Y, Okamoto T, Yoshida A. Therapeutic strategy for differentiated thyroid carcinoma in Japan based on a newly established guideline managed by Japanese Society of Thyroid Surgeons and Japanese Association of Endocrine Surgeons. *World J Surg*. (2011) 35:111–21. doi: 10.1007/s00268-010-0832-6
- Ling Y, Zhang L, Li K, Zhao Y, Zhao J, Jia L, et al. Carbon nanoparticle-guided intraoperative lymph node biopsy predicts the status of lymph nodes posterior to right recurrent laryngeal nerve in cN0 papillary thyroid carcinoma. *Gland Surg*. (2021) 10:1554–63. doi: 10.21037/gts-20-920
- Khokhar MT, Day KM, Sangal RB, Ahmedli NN, Pisharodi LR, Beland MD, et al. Preoperative high-resolution ultrasound for the assessment of Malignant central compartment lymph nodes in papillary thyroid cancer. *Thyroid*. (2015) 25:1351–4. doi: 10.1089/thy.2015.0176
- Kim SK, Park I, Woo JW, Lee JH, Choe JH, Kim JH, et al. Predictive factors for lymph node metastasis in papillary thyroid microcarcinoma. *Ann Surg Oncol*. (2016) 23:2866–73. doi: 10.1245/s10434-016-5225-0
- Cho SY, Lee TH, Ku YH, Kim HI, Lee GH, Kim MJ. Central lymph node metastasis in papillary thyroid microcarcinoma can be stratified according to the number, the size of metastatic foci, and the presence of desmoplasia. *Surgery*. (2015) 157:111–8. doi: 10.1016/j.surg.2014.05.023
- Jiwang L, Yahong L, Kai L, Bo H, Yuejiao Z, Haotian W, et al. Clinicopathologic factors and preoperative ultrasonographic characteristics for predicting central lymph node metastasis in papillary thyroid microcarcinoma: a single center retrospective study. *Braz J Otorhinolaryngol*. (2022) 88:36–45. doi: 10.1016/j.bjorl.2020.05.004
- Yang Z, Heng Y, Lin J, Lu C, Yu D, Tao L, et al. Nomogram for predicting central lymph node metastasis in papillary thyroid cancer: A retrospective cohort study of two clinical centers. *Cancer Res Treat*. (2020) 52:1010–8. doi: 10.4143/crt.2020.254
- Bae MR, Nam SH, Roh JL, Choi SH, Nam SY, Kim SY. Thyroid stimulating hormone suppression and recurrence after thyroid lobectomy for papillary thyroid carcinoma. *Endocrine*. (2022) 75:487–94. doi: 10.1007/s12020-021-02911-x
- Li M, Zheng R, Dal Maso L, Zhang S, Wei W, Vaccarella S. Mapping overdiagnosis of thyroid cancer in China. *Lancet Diabetes Endocrinol*. (2021) 9:330–2. doi: 10.1016/S2213-8587(21)00083-8
- Miranda-Filho A, Lortet-Tieulent J, Bray F, Cao B, Franceschi S, Vaccarella S, et al. Thyroid cancer incidence trends by histology in 25 countries: a population-based study. *Lancet Diabetes Endocrinol*. (2021) 9:225–34. doi: 10.1016/S2213-8587(21)00027-9
- Kebebew E, Clark OH. Differentiated thyroid cancer: “complete” rational approach. *World J Surg*. (2000) 24:942–51. doi: 10.1007/s002680010165
- Chen AY, Jemal A, Ward EM. Increasing incidence of differentiated thyroid cancer in the United States, 1988–2005. *Cancer*. (2009) 115:3801–7. doi: 10.1002/cncr.24416
- Akin S, Yazgan Aksoy D, Akin S, Kılıç M, Yetişir F, Bayraktar M. Prediction of central lymph node metastasis in patients with thyroid papillary microcarcinoma. *Turk J Med Sci*. (2017) 47:1723–7. doi: 10.3906/sag-1702-99
- Holoubek SA, Yan H, Khokar AH, Kuchta KM, Winchester DJ, Prinz RA, et al. Aggressive variants of papillary thyroid microcarcinoma are associated with high-risk features, but not decreased survival. *Surgery*. (2020) 167:19–27. doi: 10.1016/j.surg.2019.03.030
- Kuo EJ, Goffredo P, Sosa JA, Roman SA. Aggressive variants of papillary thyroid microcarcinoma are associated with extrathyroidal spread and lymph-node metastases: a population-level analysis. *Thyroid*. (2013) 23:1305–11. doi: 10.1089/thy.2012.0563
- Hyun SM, Song HY, Kim SY, Nam SY, Roh JL, Han MW, et al. Impact of combined prophylactic unilateral central neck dissection and hemithyroidectomy in patients with papillary thyroid microcarcinoma. *Ann Surg Oncol*. (2012) 19:591–6. doi: 10.1245/s10434-011-1995-6
- Zhang L, Liu Z, Liu Y, Gao W, Zheng C. The clinical prognosis of patients with cN0 papillary thyroid microcarcinoma by central neck dissection. *World J Surg Oncol*. (2015) 13:138. doi: 10.1186/s12957-015-0553-2
- Yu X, Song X, Sun W, Zhao S, Zhao J, Wang YG. Independent risk factors predicting central lymph node metastasis in papillary thyroid microcarcinoma. *Horm Metab Res*. (2017) 49:201–7. doi: 10.1055/s-0043-101917
- Ito Y, Tomoda C, Uruno T, Takamura Y, Miya A, Kobayashi K, et al. Preoperative ultrasonographic examination for lymph node metastasis: usefulness when designing lymph node dissection for papillary microcarcinoma of the thyroid. *World J Surg*. (2004) 28:498–501. doi: 10.1007/s00268-004-7192-z
- Choi YJ, Yun JS, Kook SH, Jung EC, Park YL. Clinical and imaging assessment of cervical lymph node metastasis in papillary thyroid carcinomas. *World J Surg*. (2010) 34:1494–9. doi: 10.1007/s00268-010-0541-1
- Thompson AM, Turner RM, Hayen A, Aniss A, Jalaty S, Learoyd DL, et al. A preoperative nomogram for the prediction of ipsilateral central compartment lymph node metastases in papillary thyroid cancer. *Thyroid*. (2014) 24:675–82. doi: 10.1089/thy.2013.0224
- Fu AZ, Cantor SB, Kattan MW. Use of nomograms for personalized decision-analytic recommendations. *Med Decis Making*. (2010) 30:267–74. doi: 10.1177/0272989X09342278
- Specht MC, Kattan MW, Gonen M, Fey J, Van Zee KJ. Predicting nonsentinel node status after positive sentinel lymph biopsy for breast cancer: clinicians versus nomogram. *Ann Surg Oncol*. (2005) 12:654–9. doi: 10.1245/ASO.2005.06.037
- Ross YL, Gerigk C, Gonen M, Yossepowitch O, Caggiannos I, Sogani PC, et al. Comparisons of nomograms and urologists' predictions in prostate cancer. *Semin Urol Oncol*. (2002) 20:82–8. doi: 10.1053/suro.2002.32490
- Yang Y, Chen C, Chen Z, Jiang J, Chen Y, Jin L, et al. Prediction of central compartment lymph node metastasis in papillary thyroid microcarcinoma. *Clin Endocrinol (Oxf)*. (2014) 81:282–8. doi: 10.1111/cen.12417
- Wang Y, Guan Q, Xiang J. Nomogram for predicting central lymph node metastasis in papillary thyroid microcarcinoma: A retrospective cohort study of 8668 patients. *Int J Surg*. (2018) 55:98–102. doi: 10.1016/j.ijsu.2018.05.023
- Sun J, Jiang Q, Wang X, Liu W, Wang X. Nomogram for preoperative estimation of cervical lymph node metastasis risk in papillary thyroid microcarcinoma. *Front Endocrinol (Lausanne)*. (2021) 12:613974. doi: 10.3389/fendo.2021.613974
- Lim YC, Choi EC, Yoon YH, Kim EH, Koo BS. Central lymph node metastases in unilateral papillary thyroid microcarcinoma. *Br J Surg*. (2009) 96:253–7. doi: 10.1002/bjs.6484
- Kim YS. Patterns and predictive factors of lateral lymph node metastasis in papillary thyroid microcarcinoma. *Otolaryngol Head Neck Surg*. (2012) 147:15–9. doi: 10.1177/0194599812439277
- Choi WR, Roh JL, Gong G, Cho KJ, Choi SH, Nam SY, et al. Multifocality of papillary thyroid carcinoma as a risk factor for disease recurrence. *Oral Oncol*. (2019) 94:106–10. doi: 10.1016/j.oraloncology.2019.05.023
- Kim JW, Roh JL, Gong G, Cho KJ, Choi SH, Nam SY, et al. Extent of extrathyroidal extension as a significant predictor of nodal metastasis and extranodal extension in patients with papillary thyroid carcinoma. *Ann Surg Oncol*. (2017) 24:460–8. doi: 10.1245/s10434-016-5594-4
- Lango M, Flieder D, Arrangoiz R, Veloski C, Yu JQ, Li T, et al. Extranodal extension of metastatic papillary thyroid carcinoma: correlation with biochemical endpoints, nodal persistence, and systemic disease progression. *Thyroid*. (2013) 23:1099–105. doi: 10.1089/thy.2013.0027
- Zhang L, Ling Y, Zhao Y, Li K, Zhao J, Kang H. A nomogram based on clinicopathological and ultrasound imaging characteristics for predicting cervical lymph node metastasis in cN0 unilateral papillary thyroid microcarcinoma. *Front Surg*. (2021) 8:742328. doi: 10.3389/fsurg.2021.742328

45. Mohamed HE, Mohamed SE, Anwar MA, Al-Qurayshi Z, Sholl A, Thethi T, et al. The significance of enlarged cervical lymph nodes in diagnosing thyroid cancer. *J Cancer Res Ther.* (2016) 12:1006–9. doi: 10.4103/0973-1482.171360
46. Hands KE, Cervera A, Fowler LJ. Enlarged benign-appearing cervical lymph nodes by ultrasonography are associated with increased likelihood of cancer somewhere within the thyroid in patients undergoing thyroid nodule evaluation. *Thyroid.* (2010) 20:857–62. doi: 10.1089/thy.2009.0464
47. Zhang TT, Qi XZ, Chen JP, Shi RL, Wen SS, Wang YL, et al. The association between tumor's location and cervical lymph nodes metastasis in papillary thyroid cancer. *Gland Surg.* (2019) 8:557–68. doi: 10.21037/gs.2019.10.02
48. Lee YS, Shin SC, Lim YS, Lee JC, Wang SG, Son SM, et al. Tumor location-dependent skip lateral cervical lymph node metastasis in papillary thyroid cancer. *Head Neck.* (2014) 36:887–91. doi: 10.1002/hed.23391
49. Liu N, Chen B, Li L, Zeng Q, Sheng L, Zhang B, et al. Effect of tumor location on the risk of bilateral central lymph node metastasis in unilateral 1–4 cm papillary thyroid carcinoma. *Cancer Manag Res.* (2021) 13:5803–12. doi: 10.2147/CMAR.S318076
50. Feng JW, Hong LZ, Wang F, Wu WX, Hu J, Liu SY, et al. A nomogram based on clinical and ultrasound characteristics to predict central lymph node metastasis of papillary thyroid carcinoma. *Front Endocrinol (Lausanne).* (2021) 12:666315. doi: 10.3389/fendo.2021.666315
51. Kwak JY, Han KH, Yoon JH, Moon HJ, Son EJ, Park SH, et al. Thyroid imaging reporting and data system for US features of nodules: a step in establishing better stratification of cancer risk. *Radiology.* (2011) 260:892–9. doi: 10.1148/radiol.11110206
52. Yin L, Zhang W, Bai W, He W. Relationship between morphologic characteristics of ultrasonic calcification in thyroid nodules and thyroid carcinoma. *Ultrasound Med Biol.* (2020) 46:20–5. doi: 10.1016/j.ultrasmedbio.2019.09.005
53. Khoo ML, Asa SL, Witterick IJ, Freeman JL. Thyroid calcification and its association with thyroid carcinoma. *Head Neck.* (2002) 24:651–5. doi: 10.1002/hed.10115
54. Li Y, Piao J, Li M. Secular trends in the epidemiologic patterns of thyroid cancer in China over three decades: an updated systematic analysis of global burden of disease study 2019 data. *Front Endocrinol (Lausanne).* (2021) 12:707233. doi: 10.3389/fendo.2021.707233
55. Yao R, Chiu CG, Strugnelli SS, Gill S, Wiseman SM. Gender differences in thyroid cancer: a critical review. *Expert Rev Endocrinol Metab.* (2011) 6:215–43. doi: 10.1586/eam.11.9
56. Machens A, Hauptmann S, Dralle H. Disparities between male and female patients with thyroid cancers: sex difference or gender divide? *Clin Endocrinol (Oxf).* (2006) 65:500–5. doi: 10.1111/j.1365-2265.2006.02623.x
57. Gui CY, Qiu SL, Peng ZH, Wang M. Clinical and pathologic predictors of central lymph node metastasis in papillary thyroid microcarcinoma: a retrospective cohort study. *J Endocrinol Invest.* (2018) 41:403–9. doi: 10.1007/s40618-017-0759-y
58. Fuks A, Banjo C, Shuster J, Freedman SO, Gold P. Carcinoembryonic antigen (CEA): molecular biology and clinical significance. *Biochim Biophys Acta.* (1975) 417:123–52. doi: 10.1016/0304-419x(75)90002-5
59. Yan G, Zhou Y, Wu H, Xun H. Diagnostic value of serum cytokeratin 18, carcinoembryonic antigen, and thyroglobulin in patients with papillary thyroid carcinoma. *Clin Lab.* (2021) 67:245–50. doi: 10.7754/Clin.Lab.2020.200440
60. Kazaure HS, Roman SA, Sosa JA. The impact of age on thyroid cancer staging. *Curr Opin Endocrinol Diabetes Obes.* (2018) 25:330–4. doi: 10.1097/MED.0000000000000430
61. Ito Y, Miyauchi A, Kihara M, Higashiyama T, Kobayashi K, Miya A. Patient age is significantly related to the progression of papillary microcarcinoma of the thyroid under observation. *Thyroid.* (2014) 24:27–34. doi: 10.1089/thy.2013.0367
62. Zhao W, He L, Zhu J, Su A. A nomogram model based on the preoperative clinical characteristics of papillary thyroid carcinoma with Hashimoto's thyroiditis to predict central lymph node metastasis. *Clin Endocrinol (Oxf).* (2021) 94:310–21. doi: 10.1111/cen.14302
63. Wu C, Wang L, Chen W, Zou S, Yang A. Associations between body mass index and lymph node metastases of patients with papillary thyroid cancer: A retrospective study. *Med (Baltimore).* (2017) 96:e6202. doi: 10.1097/MD.00000000000006202
64. Verloop H, Louwerens M, Schoones JW, Kievit J, Smit JW, Dekkers OM. Risk of hypothyroidism following hemithyroidectomy: systematic review and meta-analysis of prognostic studies. *J Clin Endocrinol Metab.* (2012) 97:2243–55. doi: 10.1210/jc.2012-1063
65. Ahn D, Sohn JH, Jeon JH. Hypothyroidism following hemithyroidectomy: incidence, risk factors, and clinical characteristics. *J Clin Endocrinol Metab.* (2016) 101:1429–36. doi: 10.1210/jc.2015-3997
66. Park S, Jeon MJ, Song E, Oh HS, Kim M, Kwon H, et al. Clinical features of early and late postoperative hypothyroidism after lobectomy. *J Clin Endocrinol Metab.* (2017) 102:1317–24. doi: 10.1210/jc.2016-3597
67. Gambardella C, Offi C, Romano RM, De Palma M, Ruggiero R, Candela G, et al. Transcutaneous laryngeal ultrasonography: a reliable, non-invasive and inexpensive preoperative method in the evaluation of vocal cords motility—a prospective multicentric analysis on a large series and a literature review. *Updates Surg.* (2020) 72:885–92. doi: 10.1007/s13304-020-00728-3
68. Ruggiero R, Gubitosi A, Conzo G, Gili S, Bosco A, Pirozzi R, et al. Sutureless thyroidectomy. *Int J Surg.* (2014) 12:S189–93. doi: 10.1016/j.ijsu.2014.05.011

Glossary

PTC	papillary thyroid carcinoma
PTMC	papillary thyroid microcarcinoma
CLNM	central lymph node metastasis
LASSO	least absolute shrinkage and selection operator
BMI	body mass index
USG	ultrasonography
IH	intranodular hyperechoic
ETE	extrathyroidal extension
ECLN	enlarged central lymph nodes
ATA	American Thyroid Association
CLND	central lymph node dissection
TG	triglyceride
CHOL	cholesterol
FT3	free triiodothyronine
FT4	free thyroxine
TSH	thyroid stimulating hormone
TRAb	thyrotropin receptor antibody
TGAb	anti-thyroglobulin antibodies
TPOAb	thyroid peroxidase antibodies
Tg	thyroglobulin
AFP	alpha fetoprotein
CEA	carcinoembryonic antigen
Ct	calcitonin
CDFI	color doppler flow imaging
AJCC	American Joint Committee on Cancer
ROC	receiver operating characteristic
AUC	area under the curve
DCA	decision curve analysis
ELR	extreme low risk
LR	low risk
MR	moderate risk
HR	high risk
CI	confidence interval
OR	odds ratio